IEEE Access
Multidisciplinary | Rapid Review | Open Access Journal

Received 2 September 2023, accepted 26 October 2023, date of publication 20 November 2023,
date of current version 29 November 2023.

Digital Object Identifier 10.1109/ACCESS.2023.3335278

RESEARCH ARTICLE

Hybrid Beamforming and Resource Allocation Designs for mmWave Multi-User Massive MIMO-OFDM Systems on Uplink

HSIN-HSIANG TSENG[1], YUNG-FANG CHEN[1], (Member, IEEE), AND SHU-MING TSENG[2], (Member, IEEE)
[1]Department of Communication Engineering, National Central University, Taoyuan City 32001, Taiwan
[2]Department of Electronic Engineering, National Taipei University of Technology, Taipei City 10608, Taiwan

Corresponding author: Yung-Fang Chen (yfchen@ce.ncu.edu.tw)

This work was supported in part by the Ministry of Science and Technology, Taiwan, under Grant MOST 111-2221-E-008-041; and in part by Qualcomm through the Taiwan University Research Collaboration Project.

ABSTRACT In this paper, we investigate hybrid beamforming and resource allocation design problems for uplink millimeter wave (mmWave) multi-user (MU) massive multiple-input-multiple-output (MIMO) orthogonal frequency-division multiplexing (OFDM) systems. We propose three hybrid beamforming designs with dynamic streams assignment (DSA) integrated into the solution for the formulated resource allocation problem to maximize spectral efficiency. In the analog beamforming stage, three different designs are developed to maximize the channel gains of the equivalent baseband channel at each subcarrier, while the number of data streams is also determined for each mobile station (MS). Specifically, for the first design, the analog beamformers are designed to match the corresponding channel across the entire band for each MS. In the second one, to significantly reduce the complexity of the first design, we can completely avoid the matrix decomposition by selecting the appropriate set of array response vectors. The last design only performs singular value decomposition (SVD) on the channel of the center subcarrier to find the analog beamformers. In the digital beamforming stage, for the interference cancellation, the digital precoder and the combiner are obtained at each subcarrier using the block diagonalization (BD) and the coordinated transmit-receive processing method. We also develop fully-digital beamforming and another three hybrid beamforming schemes based on the existing algorithms as performance benchmarks. By being verified through numerical simulations, the spectral efficiency of the proposed schemes can be significantly improved after dynamically assigning the number of data streams for each MS. Moreover, simulations indicate the first and the third proposed hybrid beamforming designs can achieve a very competitive performance and even outperform the fully-digital design in some situations.

INDEX TERMS Resource allocation, hybrid beamforming, multiple user access, multiple-input-multiple-output (MIMO), orthogonal frequency-division multiplexing (OFDM), spectral efficiency.

I. INTRODUCTION

Millimeter wave (mmWave) communication has been regarded as a promising solution for the fifth-generation (5G) mobile network as it can support gigabit-per-second data rates [1], [2], [3]. However, the mmWave bands have severe propagation path loss [4], [5], [6], [7] while being compared to the traditional frequency bands. Due to the small wavelength of mmWave signals, a large number of antennas can be placed in a small volume to combat the poor propagation characteristics [8], [9]. Thus, mmWave systems and massive multiple-input-multiple-output (MIMO) technology can be integrated into future wireless communications, resulting in what are known as mmWave massive MIMO systems. For traditional MIMO systems, fully-digital beamforming is performed entirely in the digital domain, allowing for control

The associate editor coordinating the review of this manuscript and approving it for publication was Jie Tang.

TABLE 1. Comparison with prior work.

	[10], [15], [17], [18], [20]	[16]	[19]	[21]-[24]	[25]	[26], [27]	[28]-[30]	[31]	[32]-[35]	[36], [37]	[38], [39]	[40]	**Proposed**
Single-user	✓	✓	✓		✓	✓						✓	
Multi-user			✓	✓	✓		✓	✓	✓	✓	✓		✓
Single-carrier	✓	✓	✓	✓						✓	✓	✓	
Multi-carrier		✓			✓	✓	✓	✓	✓				✓
Single stream communication			✓		✓		✓	✓					
Multi-stream communication	✓	✓	✓	✓	✓	✓			✓	✓	✓	✓	✓
Fully-digital structure										✓			
Hybrid structure	✓	✓	✓	✓	✓	✓	✓	✓	✓		✓	✓	✓
Data streams assignment										✓	✓	✓	✓
Downlink			✓	✓	✓		✓	✓	✓	✓	✓		
Uplink													✓

over both the magnitude and the phase of the signals [10]. However, it requires a dedicated radio frequency (RF) chain per antenna [11], [12], [13], leading to significant hardware costs and power consumption, especially when deploying a large number of antennas, particularly at high frequencies [14]. To address the above issues, a new type of hybrid beamforming structure which only requires a small number of RF chains interfacing between a high-dimensional analog beamformer and a low-dimensional digital beamformer has been proposed for the mmWave massive MIMO systems [10]. In this structure, the analog beamformer is implemented via a low-cost phase shifter network with constant amplitude constraints, while the digital baseband beamformer is implemented by the digital signal processor (DSP), allowing for spatial multiplexing through multiple RF chains. Thus, hybrid beamforming structures enable a flexible compromise between system performance and implementation cost.

A. PRIOR WORK AND RESEARCH MOTIVATIONS

Most prior hybrid precoding and combining algorithms focused on the single-user (SU) systems [10], [15], [16], [17], [18], [19], [20] and multi-user (MU) systems [19], [21], [22], [23], [24] over narrowband mmWave channels. All aforementioned works are restricted to single-carrier transmissions. However, in practice, mmWave systems are more likely to operate on wideband channels with frequency selectivity due to the vast available bandwidth of mmWave. Therefore, orthogonal frequency-division multiplexing (OFDM) transmission has been acknowledged as a vital technology to overcome the multipath fading. Regarding the hybrid beamforming structure, since the analog beamforming is implemented by analog components in the time domain, designing a common analog beamforming shared across all the subcarriers is a major challenge for designers. A wideband system requires a joint optimization of performance metric across all subcarriers. Since the analog beamforming vector is independent of frequency, finding the optimal analog beamforming is harder in a wideband system compared to single-carrier systems.

Several recent works have been proposed for SU-MIMO-OFDM systems [16], [25], [26], [27], and MU multiple-input single output OFDM (MU-MISO-OFDM) systems [25], [28], [29], [30]. Different from [25], [28], [29], and [30], where they focus on the single antenna configuration for mobile station (MS), the design of hybrid beamforming for MU-MIMO-OFDM systems has been investigated in [31]. However, in [31], only analog beamforming is employed at the MS, which implies that the base station (BS) communicates to each MS via only one data stream. More practically, a small number of papers considered the multi-stream MU-MIMO-OFDM, such as [32], [33], [34], and [35].

When the users have multiple RF chains, [36], [37] indicate that the numbers of data streams can be dynamically assigned to users, thereby substantially improving system performance. Fewer papers have introduced this idea into either fully-digital or hybrid beamforming structures. The designs in [36] and [37] consider the fully-digital structure, making them unsuitable for direct application to mmWave hybrid beamforming systems due to hardware constraints. Although the idea of data streams assignment is also integrated into the existing hybrid beamforming designs [38], [39], [40], their methods were developed based on the single-carrier systems.

Moreover, although downlink transmission has been investigated in most of the aforementioned works, both the downlink and the uplink directions are of equal importance in 5G [41]. Based on the above discussion, one direct motivation is to design a more practical hybrid beamforming algorithm

integrated into the solution for the formulated resource allocation problem to maximize spectral efficiency for uplink mmWave MU and multi-stream OFDM transmission. The comparison between the proposed work with the prior work reviewed in the above is summarized in Table 1.

B. CONTRIBUTIONS

Our main contributions are summarized as follows:

- A more flexible setting is considered, where each MS can be assigned a different number of transmitted data streams, limited by the number of its RF chains. Such an idea is more advantageous to achieve better performance.
- A two-stage approach is used to design the analog and the digital beamformers separately. Three analog beamformer designs together with our allocation framework are proposed to maintain the desired signal quality and optimize the number of transmitted data streams for different MSs. For the digital beamformers, inspired by the block diagonalization (BD) and the coordinated transmit-receive processing, the digital precoders and the combiner are derived to diagonalize the equivalent MU MIMO channel composed of the analog precoders, the full-dimensional channels, and the analog combiner at each subcarrier simultaneously. Therefore, this method provides the inter-user interference-free and the inter-stream interference-free transmission. Our proposed digital beamforming design also solves the limitation on the number of users as the classic BD method does. This implies that that our proposed schemes have more flexibility in serving the number of users.
- We modify and extend three existing hybrid beamforming schemes while incorporating the idea of the variable number of data streams into these methods. In addition, they can also be used as performance benchmarks to compare against the proposed schemes.

C. ORGANIZATION AND NOTATIONS

The rest of this paper is organized as follows. In Section II, the system model, the wideband channel model, and the problem formulation are introduced. In Section III, we propose three hybrid beamforming designs with data streams assignment and modify the fully-digital and the three other existing hybrid beamforming schemes for the performance comparison. The computational complexity of the proposed and benchmark schemes is analyzed in Section IV. Simulation results are presented in Section V, and finally, in Section VI, we conclude this paper.

The following notations are used throughout this paper. Boldface upper-case letter $\boldsymbol{A}$, boldface lower-case letter $\mathbf{a}$ and lightface lower-case letter a represent a matrix, a column vector and a scalar, respectively. The transpose, Hermitian transpose, Frobenious norm, trace and rank of $\mathbf{A}$ are expressed as $\mathbf{A}^T$, $\mathbf{A}^H$, $\|\mathbf{A}\|_{\mathrm{F}}$, Tr $(\mathbf{A})$ and rank $(\mathbf{A})$, respectively. In addition, the Euclidean norm of $\mathbf{a}$ is expressed as $\|\mathbf{a}\|$. $\mathbf{A}(:, n)$, $\mathbf{A}(m, :)$ and $\mathbf{A}(m, n)$ respectively denote the n-th column vector, the m-th row vector and the element in the m-th row and n-th column of $\mathbf{A}$. $\mathbf{A}(:, m:n)$ represents the submatrix consisting of vectors from the m-th to n-th column of $\mathbf{A}$. $\angle\mathbf{A}$ is the phase of each entry in $\mathbf{A}$. The amplitude of a is denoted by $|a|$. $diag(\mathbf{a})$ returns a diagonal matrix whose diagonal entries depend on the elements of $\mathbf{a}$. $\mathbf{I}_N$ stands for the $N \times N$ identity matrix. $\mathbb{C}^{m\times n}$ describes the set of complex valued $m \times n$ matrix. $\mathbb{E}[\cdot]$ and $\mathcal{CN}(\mu, \sigma^2)$ represent the statistical expectation operator and the complex Gaussian distribution with mean μ and variance σ^2, respectively. $\min\{a_1, a_2, \cdots, a_n\}$ returns the smallest number among $a_1, a_2, \cdots, a_n$. Finally, $\mathcal{O}(\cdot)$ is the big O notation for the complexity analysis. The key system-related mathematical notations appearing in this paper are listed in Table 2.

TABLE 2. System-related notations.

Notations	Description
N_{BS}	Number of antennas at the BS
N_{RF}^{BS}	Number of RF chains at the BS
U	Number of served MSs
N_{MS}	Number of antennas at the MS
N_{RF}^{MS}	Number of RF chains at the MS
K	Number of subcarriers for OFDM system
N_s	Total number of received data streams at the BS
$n_{s,u}$	Number of transmitted data streams at the u-th MS
$\boldsymbol{s}_u[k] \in \mathbb{C}^{n_{s,u}\times 1}$	Transmitted data symbol vector of the u-th MS at the k-th subcarrier
$\mathbf{P}_u[k] \in \mathbb{C}^{n_{s,u}\times n_{s,u}}$	Diagonal power allocation matrix of the u-th MS at the k-th subcarrier
$\mathbf{F}_{\mathrm{BB},u}[k] \in \mathbb{C}^{N_{RF}^{MS}\times n_{s,u}}$	Digital precoder matrix of the u-th MS at the k-th subcarrier
$\mathbf{F}_{\mathrm{RF},u} \in \mathbb{C}^{N_{MS}\times N_{RF}^{MS}}$	Analog precoder matrix of the u-th MS
$\mathbf{H}_u[k] \in \mathbb{C}^{N_{BS}\times N_{MS}}$	Frequency domain channel matrix between the BS and the u-th MS at the k-th subcarrier
$\mathbf{n}[k] \in \mathbb{C}^{N_{BS}\times 1}$	Complex additive white Gaussian noise (AWGN) vector at the k-th subcarrier
$\mathbf{W}_{\mathrm{RF}} \in \mathbb{C}^{N_{BS}\times N_{RF}^{BS}}$	Analog combiner matrix of the BS
$\mathbf{W}_{\mathrm{BB}}[k] \in \mathbb{C}^{N_{RF}^{BS}\times N_s}$	Digital combiner matrix of the BS at the k-th subcarrier

II. SYSTEM MODEL, CANNEL MODEL, AND PROBLEM FORMULATION

A. SYSTEM MODEL

Fig. 1 describes a single cell uplink mmWave MU massive MIMO-OFDM system with perfect synchronization. Both the BS and the MSs are assumed to adopt the fully-connected hybrid beamforming structure, where each RF chain connects to all antenna elements through a phase shifter network. For OFDM, the BS is equipped with N_{BS} antennas and N_{RF}^{BS} RF chains to serve U MSs equipped with N_{MS} antennas and N_{RF}^{MS} RF chains through K subcarriers. Moreover, at the BS, the

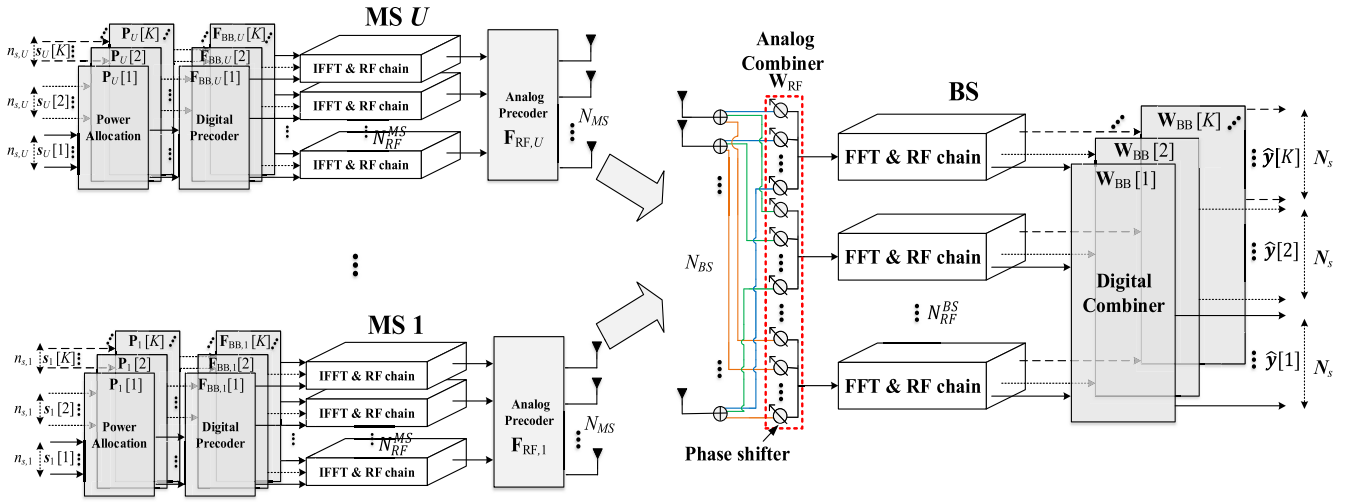

FIGURE 1. Block diagram of a single cell uplink mmWave MU massive MIMO-OFDM system with a fully-connected hybrid beamforming structure.

total number of received data streams N_s is upper bounded by the number of RF chains, i.e., $N_s \leq N_{RF}^{BS}$. The system can assign different numbers of transmitted data streams to MSs according to the channel state information (CSI) of each MS. We assume that the u-th MS can transmit $n_{s,u}$ parallel data streams at each subcarrier simultaneously, and $N_s = \sum_{u=1}^{U} n_{s,u}$ is held. Note that this system satisfies $N_s \leq N_{RF}^{BS} \ll N_{BS}$ for the BS and $n_{s,u} \leq N_{RF}^{MS} \leq N_{MS}$ for each MS to ensure the effectiveness of the transmission.

We denote by $\boldsymbol{s}_u[k] = \left[s_{u,1}[k], s_{u,2}[k], \cdots, s_{u,n_{s,u}}[k]\right]^T \in \mathbb{C}^{n_{s,u}\times 1}$ the transmitted data symbol vector of the u-th MS at the k-th subcarrier with $\mathbb{E}\left[\boldsymbol{s}_u[k]\boldsymbol{s}_u[k]^H\right] = \mathbf{I}_{n_{s,u}}$. At the u-th MS, the transmitted data symbol $\boldsymbol{s}_u[k]$ at each subcarrier first passes through a diagonal power allocation matrix $\mathbf{P}_u[k] \in \mathbb{C}^{n_{s,u}\times n_{s,u}}$ and then is precoded by a digital precoder $\mathbf{F}_{\mathrm{BB},u}[k] = [\mathbf{f}_{\mathrm{BB},u,1}[k], \mathbf{f}_{\mathrm{BB},u,2}[k], \cdots, \mathbf{f}_{\mathrm{BB},u,n_{s,u}}[k]]$, where $\mathbf{f}_{\mathrm{BB},u,n_{s,u}}[k] \in \mathbb{C}^{N_{RF}^{MS}\times 1}$ represents the digital precoder associated with the $n_{s,u}$-th data stream of the u-th MS at the k-th subcarrier. Next, the processed signals are transformed from the frequency domain to the time domain through the $N_{RF}^{MS}K$-points inverse fast Fourier transforms (IFFTs). After adding cyclic prefixes (CP), the processed signal is precoded by a common analog precoder $\mathbf{F}_{\mathrm{RF},u} \in \mathbb{C}^{N_{MS}\times N_{RF}^{MS}}$. Considering a block fading channel model, the received signal of the BS at the k-th subcarrier is

$$\mathbf{y}[k] = \sum_{u=1}^{U} \mathbf{H}_u[k]\mathbf{F}_{\mathrm{RF},u}\mathbf{F}_{\mathrm{BB},u}[k]\mathbf{P}_u[k]\boldsymbol{s}_u[k] + \mathbf{n}[k], \quad (1)$$

where $\mathbf{H}_u[k] \in \mathbb{C}^{N_{BS}\times N_{MS}}$ is the frequency domain channel matrix between the BS and the u-th MS at the k-th subcarrier, and $\mathbf{n}[k] \in \mathbb{C}^{N_{BS}\times 1} \sim \mathcal{CN}(\mathbf{0}, \sigma_n^2\mathbf{I}_{N_{BS}})$ is the complex additive white Gaussian noise (AWGN) vector in which σ_n^2 is noise power at the k-th subcarrier. At the BS, the received signal is initially combined by a common analog combiner $\mathbf{W}_{\mathrm{RF}} \in \mathbb{C}^{N_{BS}\times N_{RF}^{BS}}$ in the time domain, and then the CP removal and the $N_{RF}^{BS}K$-points fast Fourier transform (FFT) operations are applied to recover the frequency domain signals. After that, the signal at each subcarrier is combined by a low-dimensional digital combiner $\mathbf{W}_{\mathrm{BB}}[k] = \left[\mathbf{W}_{\mathrm{BB},1}[k], \mathbf{W}_{\mathrm{BB},2}[k], \cdots, \mathbf{W}_{\mathrm{BB},U}[k]\right]$, where $\mathbf{W}_{\mathrm{BB},u}[k] \in \mathbb{C}^{N_{RF}^{BS}\times n_{s,u}}$ is a low-dimension digital combiner associated with the u-th MS at the k-th subcarrier. As a result, the final processed signal at the k-th subcarrier $\hat{\mathbf{y}}[k] = \left[\hat{\mathbf{y}}_1^T[k], \hat{\mathbf{y}}_2^T[k], \cdots, \hat{\mathbf{y}}_U^T[k]\right]^T$, where $\hat{\mathbf{y}}_u[k] \in \mathbb{C}^{n_{s,u}\times 1}$, is given by

$$\hat{\mathbf{y}}[k] = \mathbf{W}_{\mathrm{BB}}^H[k]\mathbf{W}_{\mathrm{RF}}^H \sum_{u=1}^{U} \mathbf{H}_u[k]\mathbf{F}_{\mathrm{RF},u}\mathbf{F}_{\mathrm{BB},u}[k]\mathbf{P}_u[k]\boldsymbol{s}_u[k] + \mathbf{W}_{\mathrm{BB}}^H[k]\mathbf{W}_{\mathrm{RF}}^H\mathbf{n}[k]. \quad (2)$$

From (2), the final processed signal for the i-th data stream of the u-th MS at the k-th subcarrier is written as (see (3)), shown at the bottom of the next page, where $\mathbf{F}_u[k] = \mathbf{F}_{\mathrm{RF},u}\mathbf{F}_{\mathrm{BB},u}[k] \in \mathbb{C}^{N_{MS}\times n_{s,u}}$ and $\mathbf{W}_u[k] = \mathbf{W}_{\mathrm{RF}}\mathbf{W}_{\mathrm{BB},u}[k] \in \mathbb{C}^{N_{BS}\times n_{s,u}}$ respectively represent the hybrid precoder and the combiner for the u-th MS at the k-th subcarrier, and $\mathrm{P}_{u,i}[k]$ is the power allocated to the i-th data stream of the u-th MS at the k-th subcarrier. The signal-to-interference-plus-noise ratio (SINR) of $\hat{\mathbf{y}}_{u,i}[k]$ can be defined as

$$\mathrm{SINR}_{u,i}[k] = \frac{\mathrm{S}_{u,i}[k]}{\mathrm{I}_{u,i}[k] + \mathrm{N}_{u,i}[k]}, \quad (4)$$

with $\mathrm{S}_{u,i}[k]$, $\mathrm{I}_{u,i}[k]$ and $\mathrm{N}_{u,i}[k]$ being, respectively the desired signal power, interference power, and noise power, which are shown at the bottom of the next page.

B. CHANNEL MODEL

We adopt a clustered channel model with N_{cl} clusters with time delay and N_{ray} propagation paths within each cluster for simulation [42]. For OFDM systems, the frequency-domain

channel between the BS and the u-th MS at the k-th subcarrier is given by [16] and [25]

$$\mathbf{H}_u[k] = \sqrt{\frac{1}{PL_u}} \sum_{c=0}^{N_{cl}-1} \sum_{l=1}^{N_{ray}} \alpha_{u,c,l} \boldsymbol{a}_r\left(\phi^r_{u,c,l}\right) \boldsymbol{a}_t^H\left(\phi^t_{u,c,l}\right) e^{-j2\pi c(k/K)}, \tag{5}$$

where PL_u is the path loss, and $\alpha_{u,c,l} \sim \mathcal{CN}(0, \frac{N_{MS}N_{BS}}{N_{cl}N_{ray}})$, $\phi^r_{u,c,l}$ and $\phi^t_{u,c,l}$ are the complex path gain, angle of arrival (AOA), and angle of departure (AOD) of the l-th propagation path in the c-th cluster, respectively; $\boldsymbol{a}_r(\cdot)$ and $\boldsymbol{a}_t(\cdot)$ are the antenna array response vector (AARV) for the receiver and the transmitter, respectively. In our paper, a uniform linear array (ULA) with N antennas is adopted. The normalized AARV can be expressed as

$$\boldsymbol{a}(\emptyset) = \frac{1}{\sqrt{N}}\left[1, e^{j\frac{2\pi d}{\lambda}\sin(\emptyset)}, \cdots, e^{j\frac{2\pi d(N-1)}{\lambda}\sin(\emptyset)}\right]^T \tag{6}$$

in which λ is the signal wavelength, and d is the distance between adjacent antenna elements in the antenna array. Because the wavelength among different subcarrier is not equal in wideband mmWave MIMO systems, the AARV actually changes as frequency even with the same AoAs and AODs. However, when the carrier frequency is much larger than the system bandwidth, the wavelength of each subcarrier is approximately equal [25]. As a result, $\boldsymbol{a}_r\left(\phi^r_{u,c,l}\right)$ and $\boldsymbol{a}_t(\phi^t_{u,c,l})$ in (5) are assumed to be frequency-independent. The frequency-domain channel in (5) is also written in a more compact yet equivalent matrix form as

$$\mathbf{H}_u[k] = \sqrt{\frac{1}{PL_u}} \boldsymbol{A}^r_u diag\left(\boldsymbol{\alpha}_u[k]\right) \boldsymbol{A}_u^{t^H}, \tag{7}$$

where we have:

$$\boldsymbol{A}^r_u = \left[\boldsymbol{a}_r\left(\phi^r_{u,0,1}\right), \boldsymbol{a}_r\left(\phi^r_{u,0,2}\right), \cdots, \boldsymbol{a}_r\left(\phi^r_{u,N_{cl}-1,N_{ray}}\right)\right],$$

$$\boldsymbol{A}^t_u = \left[\boldsymbol{a}_t\left(\phi^t_{u,0,1}\right), \boldsymbol{a}_t\left(\phi^t_{u,0,2}\right), \cdots, \boldsymbol{a}_t\left(\phi^t_{u,N_{cl}-1,N_{ray}}\right)\right],$$

$$\boldsymbol{\alpha}_u[k] = \left[\alpha_{u,0,1}e^{-\theta_0[k]}, \alpha_{u,0,2}e^{-\theta_0[k]}, \cdots, \alpha_{u,N_{cl}-1,N_{ray}}e^{-\theta_{N_{cl}-1}[k]}\right]^T,$$

and $\theta_c[k] = \frac{2\pi ck}{K}$.

C. PROBLEM FORMULATION

The design goal is to develop hybrid precoder and combiner designs for the uplink mmWave MU massive MIMO-OFDM system to maximize the overall spectral efficiency under the constant amplitude constraints and total transmitted power constraint of each MS for the formulated resource allocation problem. The subcarrier allocation schemes are possibly unnecessary due to the channel hardening effect, so each MS can communicate with the BS across the entire band simultaneously [43], [44]. Multiple users can be served at each subcarrier in the same time to increase the system throughput [45]. We assume that perfect CSI is available. In this case, the optimization problem can be formulated as

$$\max_{\substack{(\mathbf{F}_{\mathrm{RF},u})_{u=1'}^{U}[(\mathbf{F}_{\mathrm{BB},u}[k])_{k=1}^{K}]_{u=1'}^{U} \\ \mathbf{W}_{\mathrm{RF}'}(\mathbf{W}_{\mathrm{BB}[k]})_{k=1'}^{K} \\ (n_{s,u})_{u=1'}^{U}[(\mathbf{P}_u[k])_{k=1}^{K}]_{u=1}^{U}}} \frac{1}{K}\sum_{k=1}^{K}\sum_{u=1}^{U}\sum_{i=1}^{n_{s,u}} \times \log_2\left(1+\mathrm{SINR}_{u,i}[k]\right) \tag{8}$$

$$\text{s.t.} \quad \left|\mathbf{F}_{\mathrm{RF},u}(m,n)\right| = \frac{1}{\sqrt{N_{MS}}}, \forall u, m, n, \tag{8a}$$

$$\left|\mathbf{W}_{\mathrm{RF}}(m,n)\right| = \frac{1}{\sqrt{N_{BS}}}, \forall m, n, \tag{8b}$$

$$\sum_{k=1}^{K}\left\|\mathbf{P}_u[k]\right\|_{\mathrm{F}}^2 = P_0, \forall u, \tag{8c}$$

$$\left\|\mathbf{F}_{\mathrm{RF},u}\mathbf{f}_{\mathrm{BB},u,i}[k]\right\|^2 = 1, \forall u, i, k. \tag{8d}$$

$$\hat{\mathbf{y}}_{u,i}[k] = \mathbf{W}_u[k](:,i)^H\mathbf{H}_u[k]\mathbf{F}_u[k](:,i)\sqrt{\mathrm{P}_{u,i}[k]}s_{u,i}[k] + \sum_{l=1,l\neq i}^{n_{s,u}}\mathbf{W}_u[k](:,i)^H\mathbf{H}_u[k]\mathbf{F}_u[k](:,l)\sqrt{\mathrm{P}_{u,l}[k]}s_{u,l}[k] + \sum_{m=1,m\neq u}^{U}\sum_{l=1}^{n_{s,m}}\mathbf{W}_u[k](:,i)^H\mathbf{H}_m[k]\mathbf{F}_m[k](:,l)\sqrt{\mathrm{P}_{m,l}[k]}s_{m,l}[k] + \mathbf{W}_u[k](:,i)^H\mathbf{n}[k] \tag{3}$$

$$\mathrm{S}_{u,i}[k] = \left|\mathbf{W}_u[k](:,i)^H\mathbf{H}_u[k]\mathbf{F}_u[k](:,i)\right|^2\mathrm{P}_{u,i}[k]$$

$$\mathrm{I}_{u,i}[k] = \sum_{l=1,l\neq i}^{n_{s,u}}\left|\mathbf{W}_u[k](:,i)^H\mathbf{H}_u[k]\mathbf{F}_u[k](:,l)\right|^2\mathrm{P}_{u,l}[k] + \sum_{m=1,m\neq u}^{U}\sum_{l=1}^{n_{s,m}}\left|\mathbf{W}_u[k](:,i)^H\mathbf{H}_m[k]\mathbf{F}_m[k](:,l)\right|^2\mathrm{P}_{m,l}[k]$$

$$\mathrm{N}_{u,i}[k] = \sigma_n^2\left\|\mathbf{W}_u[k](:,i)\right\|^2$$

In addition to the design of hybrid beamforming as in most prior works, we would also determine the number of transmitted data streams for each MS and the transmitted power allocation matrix of each MS at each subcarrier. Both constraint (8a) and constraint (8b) are imposed the constant amplitude requirement on all the entries of the analog precoder for each MS and the analog combiner at BS, respectively. Constraint (8c) means that the total transmitted power of each MS is P_0. To meet (8c), $\mathbf{f}_{\mathrm{BB},u,i}[k]$ is normalized to satisfy constraint (8d). In the problem (8), joint optimization is very challenging, and the non-convex constant amplitude constraints on $\mathbf{F}_{\mathrm{RF},u}$ and $\mathbf{W}_{\mathrm{RF}}$ make finding the global optimal solution intractable [10].To simplify the difficulty of the solution process, we utilize the two-stage approach, in which the optimization of analog and digital beamformers are decoupled and solved separately similar to the approaches in [19], [21], [22], [23], [24], [25], [26], [27], [28], [29], [30], [32], [33], [34], and [35].

For practical applications with imperfect channel information due to channel estimation errors, a deducted SNR value may be employed in the formula. If practical modulations for the selection of the switching levels are considered, some margin (increment in a SNR for a target BER) is required.

III. PROPOSED HYBRID BEAMFORMING DESIGNS

This section presents three novel hybrid beamforming schemes based on the two-stage approach to solve the optimization problem (8). We first derive the digital beamforming design according to the equivalent baseband channel defined by the analog beamformers and full-dimensional channel, and then discuss three proposed analog beamforming designs. After obtaining the hybrid beamforming matrices, the transmitted power allocation matrix of each MS at each subcarrier is computed using water-filling. At the end of this section, to compare with the proposed schemes, we will briefly explain the fully-digital beamforming and another three hybrid beamforming schemes after slight modification of existing schemes.

A. DIGITAL BEAMFORMING DESIGN

In this part, we propose an uplink coordinated block diagonalization (UPCBD) as a low-dimension digital beamformer to eliminate the inter-user interference and inter-stream interference completely. This method is developed based on the ideas presented in [46] and [47]. However, these ideas cannot be directly applied to design digital beamforming for the systems and scenarios under consideration. Therefore, slight extensions and derivations are necessary. When all the analog precoders $\mathbf{F}_{\mathrm{RF},u}$ and the analog combiner $\mathbf{W}_{\mathrm{RF}}$ are found (the actual design of $\mathbf{F}_{\mathrm{RF},u}$ and $\mathbf{W}_{\mathrm{RF}}$ will be presented later), the equivalent baseband channel of the u-th MS at the k-th subcarrier is given by $\bar{\mathbf{H}}_u[k] = \mathbf{W}_{\mathrm{RF}}^H \mathbf{H}_u[k] \mathbf{F}_{\mathrm{RF},u}$. We define the equivalent baseband interference channel as

$$\tilde{\mathbf{H}}_u[k] = \left[\bar{\mathbf{H}}_1[k], \cdots, \bar{\mathbf{H}}_{u-1}[k], \bar{\mathbf{H}}_{u+1}[k], \cdots, \bar{\mathbf{H}}_U[k]\right]. \tag{9}$$

Denote the rank of $\tilde{\mathbf{H}}_u[k]$ as $\tilde{r}_u[k] = \mathrm{rank}\left(\tilde{\mathbf{H}}_u[k]\right) \leq N_{RF}^{MS}(U-1)$. Perform the SVD of $\tilde{\mathbf{H}}_u[k]$ as follows:

$$\tilde{\mathbf{H}}_u[k] = \left[\tilde{\mathbf{U}}_{u1}[k]\ \tilde{\mathbf{U}}_{u2}[k]\right] \tilde{\Sigma}_u[k] \tilde{\mathbf{V}}_u[k]^H, \tag{10}$$

where $\tilde{\mathbf{U}}_{u1}[k]$ consists of the first $\tilde{r}_u[k]$ left singular vectors, and $\tilde{\mathbf{U}}_{u2}[k]$ holds the last $N_{RF}^{BS} - \tilde{r}_u[k]$ left singular vectors corresponding to zero singular values. From the definition of SVD, the columns of $\tilde{\mathbf{U}}_{u2}[k]$ exactly form the orthogonal bases of the left null space of $\tilde{\mathbf{H}}_u[k]$, so we hope that $\mathbf{W}_{\mathrm{BB},u}[k]$ lies in the left null space of $\tilde{\mathbf{H}}_u[k]$ to eliminate all inter-user interference at each subcarrier. Through the above operation, we have

$$\tilde{\mathbf{U}}_{u2}^H[k] \bar{\mathbf{H}}_l[k] = \mathbf{0}, \quad l \neq u. \tag{11}$$

Next, we further perform SVD on $\tilde{\mathbf{U}}_{u2}^H[k] \bar{\mathbf{H}}_l[k]$, given by

$$\tilde{\mathbf{U}}_{u2}^H[k] \bar{\mathbf{H}}_u[k] = \dot{\mathbf{U}}_u[k] \dot{\Sigma}_u[k] \dot{\mathbf{V}}_u[k]^H. \tag{12}$$

Define $\dot{\mathbf{U}}_{u1}[k]$ and $\dot{\mathbf{V}}_{u1}[k]$ as the first $n_{s,u}$ columns of $\dot{\mathbf{U}}_u[k]$ and $\dot{\mathbf{V}}_u[k]$, respectively. Finally, the digital precoder $\mathbf{F}_{\mathrm{BB},u}[k]$ and the combiner $\mathbf{W}_{\mathrm{BB},u}[k]$ can be expressed as

$$\mathbf{F}_{\mathrm{BB},u}[k] = \dot{\mathbf{V}}_{u1}[k], \mathbf{W}_{\mathrm{BB},u}[k] = \tilde{\mathbf{U}}_{u2}[k] \dot{\mathbf{U}}_{u1}[k]. \tag{13}$$

Note that the condition of $N_{RF}^{BS} > \tilde{r}_u[k]$ is necessarily satisfied to ensure that the left null space of $\tilde{\mathbf{H}}_u[k]$ has a dimension greater than 0. However, the condition of $N_{RF}^{BS} = \tilde{r}_u[k]$ is inevitable in our system scenario. For downlink, coordinated transmit-receive processing is introduced to solve the similar issue as that in [46]. The general idea is to assume that the transmitter knows what beamforming algorithm is employed at the receiver in advance, and then it designs the transmit beams based on this knowledge. We try to extend this idea to uplink.

First, let $\hat{\mathbf{F}}_u[k]$ be a $N_{RF}^{MS} \times n_{s,u}$ transmit precoding matrix and define the new equivalent baseband interference channel for the u-th MS at the k-th subcarrier as follows:

$$\check{\mathbf{H}}_u[k] = \left[\overline{\overline{\mathbf{H}}}_1[k], \cdots, \overline{\overline{\mathbf{H}}}_{u-1}[k], \overline{\overline{\mathbf{H}}}_{u+1}[k], \cdots, \overline{\overline{\mathbf{H}}}_U[k]\right], \tag{14}$$

which is obtained by excluding $\overline{\overline{\mathbf{H}}}_u[k] = \bar{\mathbf{H}}_u[k] \hat{\mathbf{F}}_u[k]$. Since $\check{\mathbf{H}}_u[k]$ is a $N_{RF}^{BS} \times (N_s - n_{s,u})$ matrix, the condition of $N_{RF}^{BS} > \mathrm{rank}\left(\check{\mathbf{H}}_u[k]\right)$ will be satisfied. We can easily use $\check{\mathbf{H}}_u[k]$ in place of $\tilde{\mathbf{H}}_u[k]$ and then carry out (10), (12) and (13). But the number of transmitted data streams $n_{s,u}$ and the transmit precoding matrix $\hat{\mathbf{F}}_u[k]$ are essential to know for each MS in advanced. For the assignment of $n_{s,u}$, we will discuss in the subsequent subsection. The proper $\hat{\mathbf{F}}_u[k]$ can be chosen as the $n_{s,u}$ dominant right singular vectors of $\bar{\mathbf{H}}_u[k] = \bar{\mathbf{U}}_u[k] \bar{\Sigma}_u[k] \bar{\mathbf{V}}_u[k]^H$, i.e.,

$$\hat{\mathbf{F}}_u[k] = \bar{\mathbf{V}}_u[k](:, 1 : n_{s,u}). \tag{15}$$

Given this information, $\check{\mathbf{H}}_u[k]$ is then constructed, which can be used to obtain the digital precoder $\mathbf{F}_{\mathrm{BB},u}[k]$ and

Algorithm 1 The Proposed Digital Beamforming Design (UPCBD)

Input : $n_{s,u}$, $\mathbf{F}_{\mathrm{RF},u}$, $U = 1, 2, \cdots, U$, $\mathbf{W}_{\mathrm{RF}}$, $\mathbf{H}_u[k], u = 1, 2, \cdots, u, k = 1, 2, \cdots, k$.

1 : for $k = 1$ to k **do**
2 : for $u = 1$ to U **do**
3 : $\bar{\mathbf{H}}_u[k] = \mathbf{W}_{\mathrm{RF}}^H \mathbf{H}_u[k] \mathbf{F}_{\mathrm{RF},u}$.
4 : Calculate the SVD of $\bar{\mathbf{H}}_u[k] = \bar{\mathbf{U}}_u[k] \bar{\Sigma}_u[k] \bar{\mathbf{V}}_u[k]^H$.
5 : $\overline{\overline{\mathbf{H}}}_u[k] = \bar{\mathbf{H}}_u[k] \hat{\mathbf{F}}_u[k]$, where $\hat{\mathbf{F}}_u[k]$ is defined as (15).
6 : **end for**
7 : **for** $u = 1$ to U **do**
8 : Calculate $\check{\mathbf{H}}_u[k]$ according to (14).
9 : Calculate the SVD of $\check{\boldsymbol{H}}_u[k] = \left[\check{\mathbf{U}}_{u1}[k]\ \check{\mathbf{U}}_{u2}[k]\right] \check{\boldsymbol{\Sigma}}_u[k] \check{\mathbf{V}}_u[k]^{\boldsymbol{H}}$, where $\check{\mathbf{U}}_{u2}[k]$ is defined as the last $N_{RF}^{BS} - \mathrm{rank}\left(\check{\mathbf{H}}_u[k]\right)$ left singular vectors.
10: Calculate the SVD of $\check{\mathbf{U}}_{u2}^{\boldsymbol{H}}[k] \overline{\overline{\mathbf{H}}}_u[k] = \ddot{\mathbf{U}}_u[k] \ddot{\Sigma}_u[k] \ddot{\mathbf{V}}_u[k]^{\boldsymbol{H}}$.
Define $\ddot{\mathbf{U}}_{u1}[k]$ and $\ddot{\mathbf{V}}_{u1}[k]$ as the first $n_{s,u}$ columns of $\ddot{\mathbf{U}}_u[k]$ and $\ddot{\mathbf{V}}_u[k]$, respectively.
11: Define the unnormalized digital precoder

$$\tilde{\mathbf{F}}_{\mathrm{BB},u}[k] = \hat{\mathbf{F}}_u[k] \ddot{\mathbf{V}}_{u1}[k] = \left[\tilde{f}_{\mathrm{BB},u,1}[k], \tilde{f}_{\mathrm{BB},u,2}[k], \cdots, \tilde{f}_{\mathrm{BB},u,n_{s,u}}[k]\right].$$

12: for $i = 1$ to $n_{s,u}$ do
13: $\mathbf{f}_{\mathrm{BB},u,i}[k] = \frac{\tilde{f}_{\mathrm{BB},u,i}[k]}{\left\|\mathbf{F}_{\mathbf{RF},u} \tilde{f}_{\mathrm{BB},u,i}[k]\right\|}$.
14: **end for**
15: $\mathbf{F}_{\mathrm{BB},u}[k] = [\mathbf{f}_{\mathrm{BB},u,1}[k], \mathbf{f}_{\mathrm{BB},u,2}[k], \cdots, \mathbf{f}_{\mathrm{BB},u,n_{s,u}}[k]]$.
16: $\mathbf{W}_{\mathrm{BB},u}[k] = \check{\mathbf{U}}_{u2}[k] \ddot{\mathbf{U}}_{u1}[k]$.
17: **end for**
18: **end for**

Output: $\mathbf{F}_{\mathrm{BB},u}[k], \mathbf{W}_{\mathrm{BB},u}[k], u = 1, 2, \cdots, u, k = 1, 2, \cdots, k$.

the combiner $\mathbf{W}_{\mathrm{BB},u}[k]$. Furthermore, to fulfill the power constraints, the digital precoder $\mathbf{F}_{\mathrm{BB},u}[k]$ is computed after normalizing each column of the unnormalized digital precoder $\tilde{\mathbf{F}}_{\mathrm{BB},u}[k]$. Our proposed digital beamforming design is outlined in **Algorithm 1**.

B. ANALOG BEAMFORMING DESIGN

Herein, three analog beamforming designs are proposed and combined with the proposed digital beamforming design discussed in the previous subsection which further lead to three proposed hybrid beamforming designs with dynamic streams assignment (DSA). Next, three analog beamforming designs are developed in details below.

1) TENSOR UNFOLDING MATRIX DECOMPOSITION (TUMD)

In the following, the designs of $\mathbf{F}_{\mathrm{RF},u}$ and $\mathbf{W}_{\mathrm{RF}}$ are treated separately. We first design the analog precoder $\mathbf{F}_{\mathrm{RF},u}$ for each MS and then design the analog combiner $\mathbf{W}_{\mathrm{RF}}$ according to the high-dimensional channels and $\mathbf{F}_{\mathrm{RF},u}$, subsequently. Ignoring the interference and other beamforming matrices, the analog precoder of the u-th MS is designed to match the own channel for each subcarrier which can be formulated as

$$\max_{\mathbf{F}_{\mathrm{RF},u}} \sum_{k=1}^{K} \left\|\mathbf{H}_u[k] \mathbf{F}_{\mathrm{RF},u}\right\|_{\mathrm{F}}^2 \quad \text{s.t.} \quad \left|\mathbf{F}_{\mathrm{RF},u}(m,n)\right| = 1/\sqrt{N_{MS}}, \forall m, n. \tag{16}$$

We introduce the concept of tensor-unfolding [32] and drop the constant amplitude constraints. Then, the optimization problem (16) is converted into an unconstrained problem as

$$\max_{\mathbf{F}_{\mathrm{RF},u}} \left\|\mathbf{H}_u^{(l)} \tilde{\mathbf{F}}_{\mathrm{RF},u}\right\|_{\mathrm{F}}^2, \tag{17}$$

where $\mathbf{H}_u^{(l)} = \left[(\mathbf{H}_u[1])^T (\mathbf{H}_u[2])^T \cdots (\mathbf{H}_u[K])^T\right]^T \in \mathbb{C}^{(KN_{BS}) \times N_{MS}}$ is longitudinal tensor-unfolding of the three-dimensional matrix, and $\tilde{\mathbf{F}}_{\mathrm{RF},u}$ is an unconstrained analog precoder of the u-th MS. First, we apply eigenvalue decomposition (EVD) to $\mathbf{H}_u^{(l)H} \mathbf{H}_u^{(l)}$ as $\mathbf{H}_u^{(l)H} \mathbf{H}_u^{(l)} = \bar{\mathbf{V}}_u \bar{\mathbf{D}}_u \bar{\mathbf{V}}_u^H$, where $\bar{\mathbf{D}}_u$ is a diagonal matrix whose diagonal entries are the eigenvalues arranged in descending order, i.e., $\bar{\rho}_u^{(1)} \geq \bar{\rho}_u^{(2)} \geq \cdots \geq \bar{\rho}_u^{(N_{MS})}$, and the n-th column of $\bar{\mathbf{V}}_u$ is the eigenvector corresponding to $\bar{\rho}_u^{(n)}$. Then, the objective function in (17) is rewritten as

$$\left\|\mathbf{H}_u^{(l)} \tilde{\mathbf{F}}_{\mathrm{RF},u}\right\|_{\mathrm{F}}^2 = \mathrm{Tr}\left(\tilde{\mathbf{F}}_{\mathrm{RF},u}^H \mathbf{H}_u^{(l)H} \mathbf{H}_u^{(l)} \tilde{\mathbf{F}}_{\mathrm{RF},u}\right). \tag{18}$$

Obviously, the columns of $\tilde{\mathbf{F}}_{\mathrm{RF},u}$ can be constructed by the first N_{RF}^{MS} eigenvectors of $\mathbf{H}_u^{(l)H} \mathbf{H}_u^{(l)}$ corresponding to the N_{RF}^{MS} largest eigenvalues to maximize it for each MS, i.e.,

$$\tilde{\mathbf{F}}_{\mathrm{RF},u} = \bar{\mathbf{V}}_u\left(:, 1 : N_{RF}^{MS}\right). \tag{19}$$

However, $\tilde{\mathbf{F}}_{\mathrm{RF},u}$ does not satisfy the constant amplitude constraints. As in prior work [22], [28], $\mathbf{F}_{\mathrm{RF},u}$ is designed to be as close as $\tilde{\mathbf{F}}_{\mathrm{RF},u}$, which is given by

$$\max_{\mathbf{F}_{\mathrm{RF},u}} \left\|\tilde{\mathbf{F}}_{\mathrm{RF},u} - \mathbf{F}_{\mathrm{RF},u}\right\|_{\mathrm{F}}^2 \quad \text{s.t.} \quad \left|\mathbf{F}_{\mathrm{RF},u}(m,n)\right| = 1/\sqrt{N_{MS}}, \forall m, n, \tag{20}$$

and the solution can be obtained by

$$\mathbf{F}_{\mathrm{RF},u} = \frac{1}{\sqrt{N_{MS}}} e^{j\angle \tilde{\mathbf{F}}_{\mathrm{RF},u}}. \tag{21}$$

After getting the analog precoder $\mathbf{F}_{\mathrm{RF},u}$ of the u-th MS, the equivalent channel for the link between BS and the u-th MS at the k-th subcarrier is defined as

$$\mathbf{H}_{eq,u}[k] = \mathbf{H}_u[k] \mathbf{F}_{\mathrm{RF},u}. \tag{22}$$

Let the analog combiner $\mathbf{W}_{\mathrm{RF}}$ be represented by $\mathbf{W}_{\mathrm{RF}} = \left[\mathbf{W}_{\mathrm{RF},1}\ \mathbf{W}_{\mathrm{RF},2} \cdots \mathbf{W}_{\mathrm{RF},U}\right] \in \mathbb{C}^{N_{BS} \times \left(\sum_{u=1}^{U} N_{RF,u} = N_{RF}^{BS}\right)}$,

where $\mathbf{W}_{\mathrm{RF},u} \in \mathbb{C}^{N_{BS}\times N_{RF,u}}$ is the submatrix of $\mathbf{W}_{\mathrm{RF}}$ corresponding to the u-th MS at each subcarrier. Applying the same concept as the designs of $\mathbf{F}_{\mathrm{RF},u}$, we assume that the $N_{RF,u}$ columns of $\mathbf{W}_{\mathrm{RF}}$ are used to match the u-th MS's equivalent channel on the entire band regardless of the interference. To obtain $\mathbf{W}_{\mathrm{RF}}$, we first solve

$$\begin{aligned}\max_{(N_{RF,u},\tilde{\mathbf{W}}_{RF,u})_{u=1}^{U}} \quad & \sum_{u=1}^{U}\left\|\tilde{\mathbf{W}}_{\mathrm{RF},u}^{H}\mathbf{H}_{eq,u}^{(h)}\right\|_{\mathrm{F}}^{2}\\ \text{s.t.} \quad & \sum_{u=1}^{U}N_{RF,u}=N_{RF}^{BS},\\ & 1\le N_{RF,u},\forall u,\end{aligned} \tag{23}$$

where $\mathbf{H}_{eq,u}^{(h)} = \left[\mathbf{H}_{eq,u}[1]\ \mathbf{H}_{eq,u}[2]\ \cdots\ \mathbf{H}_{eq,u}[K]\right] \in \mathbb{C}^{N_{BS}\times(KN_{RF}^{MS})}$ is horizontal tensor-unfolding of the three-dimensional matrix, and $\tilde{\mathbf{W}}_{\mathrm{RF},u}$ is the $N_{RF,u}$ columns of the unconstrained analog combiner $\tilde{\mathbf{W}}_{\mathrm{RF}}$. Since $\mathbf{W}_{\mathrm{RF}}$ can be decomposed into the U different size submatrices in general, it is notable that all MSs are allocated different numbers of RF chains at the BS. To solve (23) and determine the number of transmitted data streams for each MS $\left(n_{s,u}\right)_{u=1}^{U}$, the proposed solution consists of the following two stages:

a: INITIAL RF CHAINS ALLOCATION STAGE

To begin with, we temporarily relax the total number of RF chains constraint at the BS and allocate the largest available N_{RF}^{MS} RF chains to each MS to avoid that the RF resource at the BS is dominated by one MS, so (23) can be rewritten as

$$\begin{aligned}\max_{(N_{RF,u},\tilde{\mathbf{W}}_{\mathrm{RF},u})_{u=1}^{U}} \quad & \sum_{u=1}^{U}\left\|\tilde{\mathbf{W}}_{\mathrm{RF},u}^{H}\mathbf{H}_{eq,u}^{(h)}\right\|_{\mathrm{F}}^{2}\\ \text{s.t.} \quad & \sum_{u=1}^{U}N_{RF,u}\le N_{RF}^{BS},\\ & 1\le N_{RF,u}\le N_{RF}^{MS},\forall u.\end{aligned} \tag{24}$$

We perform EVD on $\mathbf{H}_{eq,u}^{(h)}\mathbf{H}_{eq,u}^{(h)H}$ as $\mathbf{H}_{eq,u}^{(h)}\mathbf{H}_{eq,u}^{(h)H} = \bar{\mathbf{U}}_{eq,u}\bar{\mathbf{D}}_{eq,u}\bar{\mathbf{U}}_{eq,u}^{H}$, where $\bar{\mathbf{D}}_{eq,u}$ is a diagonal matrix whose diagonal entries are the eigenvalues arranged in descending order, i.e., $\bar{\rho}_{eq,u}^{(1)} \ge \bar{\rho}_{eq,u}^{(2)} \ge \cdots \ge \bar{\rho}_{eq,u}^{(N_{BS})}$, and the n-th column of $\bar{\mathbf{U}}_{eq,u}$ is the eigenvector corresponding to $\bar{\rho}_{eq,u}^{(n)}$. By comparing $\left\|\tilde{\mathbf{W}}_{\mathrm{RF},u}^{H}\mathbf{H}_{eq,u}^{(h)}\right\|_{\mathrm{F}}^{2}$ with the objective function in (17), their mathematic forms are similar in nature. We know that the columns of $\tilde{\mathbf{W}}_{\mathrm{RF},u}$ can be constructed by the first to $N_{RF,u}$-th columns of $\bar{\mathbf{U}}_{eq,u}$, i.e., $\tilde{\mathbf{W}}_{\mathrm{RF},u} = \bar{\mathbf{U}}_{eq,u}\left(:, 1:N_{RF,u}\right)$. Therefore, the objective function in (24) is rewritten as $\sum_{u=1}^{U}\left\|\tilde{\mathbf{W}}_{\mathrm{RF},u}^{H}\mathbf{H}_{eq,u}^{(h)}\right\|_{\mathrm{F}}^{2} = \sum_{u=1}^{U}\sum_{n=1}^{N_{RF,u}}\bar{\rho}_{eq,u}^{(n)}$ by applying the properties of the Frobenious norm and the trace. Next, we introduce one allocation framework to decide $\left(N_{RF,u}\right)_{u=1}^{U}$. The largest number of allocated RF chains for each MS $\left(N_{RF,u}\right)_{u=1}^{U}$ is limited by N_{RF}^{MS} in this stage. To this end,

Algorithm 2 The Proposed Analog Beamforming Design (*TUMD*)

Input: $\mathbf{H}_u[k], u=1,2,\cdots,U, k=1,2,\cdots,k, N_{RF}^{MS}, N_{RF}^{BS}$.
1 : for $u=1$ to U do
2 : $\quad \mathbf{H}_u^{(l)} = \left[(\mathbf{H}_u[1])^T\ (\mathbf{H}_u[2])^T\ \cdots\ (\mathbf{H}_u[k])^T\right]^T$.
3 : $\quad$ Calculate the EVD of $\mathbf{H}_u^{(l)H}\mathbf{H}_u^{(l)} = \bar{\mathbf{V}}_u\bar{\mathbf{D}}_u\bar{\mathbf{V}}_u^H$.
4 : $\quad \mathbf{F}_{RF,u} = \frac{1}{\sqrt{N_{MS}}}e^{j\angle\bar{\mathbf{V}}_u(:,1:N_{RF}^{MS})}$.
5 : $\quad \mathbf{H}_{eq,u}^{(h)} = \left[\mathbf{H}_{eq,u}[1]\ \mathbf{H}_{eq,u}[2]\ \cdots\ \mathbf{H}_{eq,u}[k]\right]$, where $\mathbf{H}_{eq,u}[k]$ is defined as (22).
6 : $\quad$ Calculate the EVD of $\mathbf{H}_{eq,u}^{(h)}\mathbf{H}_{eq,u}^{(h)H} = \bar{\mathbf{U}}_{eq,u}\bar{\mathbf{D}}_{eq,u}\bar{\mathbf{U}}_{eq,u^H}$.
7 : **end for**
Initial RF chains allocation stage
8 : Assign one RF chain to all served MSs, i.e., $N_{RF,u}=1, u=1,2,\cdots,U$.
9 : **repeat**
10: $\quad u^* = \underset{u\in C}{\operatorname{argmax}}\ \bar{\rho}_{eq,u}^{(N_{RF,u}+1)}$.
11: $\quad N_{RF,u^*} = N_{RF,u^*}+1$.
12: **until** $\sum_{u=1}^{U}N_{RF,u}=N_{RF}^{BS}$ or $C=\emptyset$
13: $n_{s,u}=N_{RF,u}, u=1,2,\cdots,U$.
Extra RF chains allocation stage
14: **if** $\sum_{u=1}^{U}N_{RF,u} < N_{RF}^{BS}$ **then**
15: $\quad$ **repeat**
16: $\quad u^* = \underset{u\in\{1,2,\cdots,U\}}{\operatorname{argmax}}\ \bar{\rho}_{eq,u}^{(N_{RF,u}+1)}$.
17: $\quad N_{RF,u^*} = N_{RF,u^*}+1$.
18: $\quad$ **until** $\sum_{u=1}^{U}N_{RF,u}=N_{RF}^{BS}$
19: **end if**
20: **for** $u=1$ to U **do**
21: $\quad \mathbf{W}_{RF,u} = \frac{1}{\sqrt{N_{BS}}}e^{j\angle\bar{\mathbf{U}}_{eq,u}(:,1:N_{RF,u})}$.
22: **end for**
23: $\mathbf{W}_{RF} = \left[\mathbf{W}_{\mathrm{RF},1}\ \mathbf{W}_{\mathrm{RF},2}\ \cdots\ \mathbf{W}_{\mathrm{RF},U}\right]$.
Output: $\mathbf{F}_{\mathrm{RF},u}, n_{s,u}, u=1,2,\cdots,U$ and $\mathbf{W}_{\mathrm{RF}}$.

we define a candidate MSs' index set C as

$$C=\left\{u|N_{RF,u}<N_{RF}^{MS}, u\in U\right\},\ \text{where}\ \mathcal{U}=\{1,2,\cdots,\mathcal{U}\}. \tag{25}$$

Meanwhile, each served MS is initially assigned one RF chain. Then, based on the selection rule in (26),

$$u^* = \underset{u\in c}{\operatorname{argmax}}\ \bar{\rho}_{eq,u}^{(N_{RF,u}+1)} \tag{26}$$

we successively select one MS u^* from the set C and add one RF chain to it until the condition of the total number of allocated RF chains equal to N_{RF}^{BS} are reached, i.e., $\sum_{u=1}^{U}N_{RF,u}=N_{RF}^{BS}$ or the set C becomes an empty set; that is, all MSs have already been assigned N_{RF}^{MS} RF chains. The analog beamformer sets the spatial beamforming direction [48]. Therefore, the result of streams assignment can be obtained from the above RF chains allocation, i.e., $\left(n_{s,u}=N_{RF,u}\right)_{u=1}^{U}$. To satisfy the constant amplitude

Algorithm 3 The Proposed Analog Beamforming Design (*SCCMD*)

Input: $\boldsymbol{\beta}_u, \boldsymbol{A}_u^t, \boldsymbol{A}_u^r, u = 1, 2, \cdots, U, N_{RF}^{MS}, N_{RF}^{BS}$.
1 : **for** $u = 1$ to U **do**
2 : Obtain $\tilde{\boldsymbol{\beta}}_u$ by sorting the elements of $\boldsymbol{\beta}_u$ in descending order and return the corresponding sort index vector i.
3 : $L = length(\boldsymbol{i})$, where $length(\boldsymbol{a})$ returns the length of $\boldsymbol{a}$.
4 : $\tilde{\boldsymbol{A}}_u^t =$ Empty matrix.
5 : $\tilde{\boldsymbol{A}}_u^r =$ Empty matrix.
6 : **for** $d = 1$ to L **do**
7 : $c = \boldsymbol{i}(d)$.
8 : $\tilde{\boldsymbol{A}}_u^t = \left[\tilde{\boldsymbol{A}}_u^t | A_u^t(:, c)\right]$.
9 : $\tilde{\boldsymbol{A}}_u^r = \left[\tilde{\boldsymbol{A}}_u^r | A_u^r(:, c)\right]$.
10: **end for**
11: $\mathbf{F}_{RF,u} = \tilde{\boldsymbol{A}}_u^t(:, 1 : N_{RF}^{MS})$.
12: **end for**
13: Obtain $N_{RF,u}$ and $n_{s,u}$ by replacing the selection rule in (26) with (29) and employing the allocation framework as Algorithm 2.
14: **for** $u = 1$ to U **do**
15: $\mathbf{W}_{\mathrm{RF},u} = \tilde{\boldsymbol{A}}_u^r(:, 1 : N_{\mathrm{RF},u})$.
16: **end for**
17: $\mathbf{W}_{\mathrm{RF}} = \left[\mathbf{W}_{\mathrm{RF},1}\ \mathbf{W}_{RF,2}\ \cdots \mathbf{W}_{\mathrm{RF},U}\ \right]$.
Output: $\mathbf{F}_{\mathrm{RF},u}, n_{s,u}, u = 1, 2, \cdots, U$ and $\mathbf{W}_{\mathrm{RF}}$.

constraints, $\mathbf{W}_{\mathrm{RF},u}$ is given by

$$\mathbf{W}_{\mathrm{RF},u} = \frac{1}{\sqrt{N_{BS}}} e^{j\angle \tilde{\mathbf{W}}_{\mathrm{RF},u}}. \tag{27}$$

b: EXTRA RF CHAINS ALLOCATION STAGE

If there are still extra RF chains resource available after the *initial RF chains allocation stage*, it implies the remaining column vectors of $\mathbf{W}_{\mathrm{RF}}$ are required to design. We can further allocate the extra RF chains to MS by using the aforementioned allocation idea and then obtain the complete $\mathbf{W}_{\mathrm{RF}}$. In conclusion, the overall steps of *TUMD* are summarized in **Algorithm 2**.

2) SIMILAR CHANNEL COVARIANCE MATRIX DECOMPOSITION (SCCMD)

Since *TUMD* requires the high-dimensional matrix decomposition when the number of subcarriers are large, it leads to the high computational complexity. In view of this, developing a relatively low complexity analog beamforming design integrated into the solution for the formulated resource allocation problem is our goal in this part, and we hope to enhance the equivalent channel gain through the analog beamformer to provide as robust transmission as possible for each stream. Here, we drop the constant amplitude constraints and impose the number of RF chains constraints as in (24) to obtain the following problem:

Algorithm 4 The Proposed Analog Beamforming Design (*Modified SCCMD*)

Input: $\mathbf{H}_u[k], u = 1, 2, \cdots, U, k = 1, 2, \cdots, k, N_{RF}^{MS}, N_{RF}^{BS}$.
1 : **for** $u = 1$ to U **do**
2 : Calculate the SVD of $\mathbf{H}_u[k/2] = \mathbf{U}_u \boldsymbol{\Sigma}_u \mathbf{V}_u^H$.
3 : $\mathbf{F}_{RF,u} = \frac{1}{\sqrt{N_{MS}}} e^{j\angle \mathbf{V}_u(:, 1:N_{RF}^{MS})}$.
4 : **end for**
5 : Obtain $N_{\mathrm{RF},u}$ and $n_{s,u}$ by replacing the selection rule in (26) or (29) with (30) and employing the allocation framework as Algorithm 2.
6 : **for** $u = 1$ to U **do**
7 : $\mathbf{W}_{\mathrm{RF},u} = \frac{1}{\sqrt{N_{BS}}} e^{j\angle \mathrm{U}_u(:, 1:N_{RF,u})}$.
8 : **end for**
9 : $\mathbf{W}_{\mathrm{RF}} = \left[\mathbf{W}_{\mathrm{RF},1}\ \mathbf{W}_{\mathrm{RF},2}\ \cdots \mathbf{W}_{\mathrm{RF},U}\ \right]$.
Output: $\mathbf{F}_{\mathrm{RF},u}, n_{s,u}, u = 1, 2, \cdots, U$ and $\mathbf{W}_{\mathrm{RF}}$.

$$\begin{aligned} \max_{(N_{RF,u}, \tilde{\mathbf{F}}_{\mathrm{RF},u}, \tilde{\mathbf{W}}_{\mathrm{RF},u})_{u=1}^{U}} \quad & \sum_{u=1}^{U} \sum_{k=1}^{K} \left\| \tilde{\mathbf{W}}_{\mathrm{RF},u}^H \mathbf{H}_u[k] \tilde{\mathbf{F}}_{\mathrm{RF},u} \right\|_{\mathrm{F}}^2 \\ \text{s.t.} \quad & \sum_{u=1}^{U} N_{RF,u} \le N_{RF}^{BS}, \\ & 1 \le N_{RF,u} \le N_{RF}^{MS}, \forall u. \end{aligned} \tag{28}$$

Because of the hardware implementation constraint, designing individual analog beamforming matrix on a per subcarrier basis is not practical. Fortunately, according to [25], by using the compact form of the channel in (7), when the number of antennas is sufficiently large, $\bar{Q}_u[k] = \mathbf{H}_u[k]^H \mathbf{H}_u[k]$ can be simplified as $\gamma \boldsymbol{A}_u^t diag\left(\boldsymbol{\beta}_u\right) \boldsymbol{A}_u^{t^H}$, where $\boldsymbol{\beta}_u = [\frac{|\alpha_{u,0,1}|^2}{PL_u}, \frac{|\alpha_{u,0,2}|^2}{PL_u}, \ldots, \frac{|\alpha_{u,N_{cl}-1,N_{ray}}|^2}{PL_u}]^T$. Hence, the eigenvectors of $\bar{\boldsymbol{Q}}_u[k]$ are approximated as the columns of $\boldsymbol{A}_u^t$ for each subcarrier. Motivated by this useful result, $\tilde{\mathbf{F}}_{\mathrm{RF},u}$ can be designed as the subset of columns of $\boldsymbol{A}_u^t$ corresponding to the N_{RF}^{MS} largest $|\alpha_{u,c,l}|^2 / PL_u$. Using the similar mathematical manipulation, $\mathbf{H}_u[k]\mathbf{H}_u[k]^H$ is simplified as $\gamma \boldsymbol{A}_u^r diag\left(\boldsymbol{\beta}_u\right) \boldsymbol{A}_u^{r^H}$, so $\tilde{\mathbf{W}}_{\mathrm{RF},u}$ is designed as the subset of columns of $\boldsymbol{A}_u^r$ corresponding to the $N_{RF,u}$ largest $|\alpha_{u,c,l}|^2 / PL_u$. So far, we know that the columns of $\tilde{\mathbf{F}}_{\mathrm{RF},u}$ and $\tilde{\mathbf{W}}_{\mathrm{RF},u}$ are selected from the columns of $\boldsymbol{A}_u^t$ and $\boldsymbol{A}_u^r$, respectively, but $\left(N_{RF,u}\right)_{u=1}^{U}$ are still required to determine.

To solve this, we sort the elements of $\boldsymbol{\beta}_u$ for each MS in descending order to obtain $\tilde{\beta}_u = [\tilde{\beta}_u^{(1)}, \tilde{\beta}_u^{(2)}, \cdots, \tilde{\beta}_u^{(N_{cl}N_{ray})}]^T$ and then employ the allocation framework as **Algorithm 2** after replacing the selection rule in (26) with

$$u^* = \underset{u \in C}{\operatorname{argmax}}\ \tilde{\beta}_u^{(N_{RF,u}+1)}. \tag{29}$$

The overall steps of *SCCMD* can be summarized in **Algorithm 3**.

3) MODIFIED SCCMD

We try to slightly modified *SCCMD* algorithm in order to achieve a trade-off between the performance and the complexity. Only the center subcarrier's channel matrix is utilized to design a common analog precoder and a combiner in this scheme. Replacing the objective function in (28) with $\sum_{u=1}^{U}\left\|\tilde{\mathbf{W}}_{\mathrm{RF},u}^{H}\mathbf{H}_u[K/2]\tilde{\mathbf{F}}_{\mathrm{RF},u}\right\|_{\mathrm{F}}^2$, the original multi-carrier system can be seen as a single-carrier system to process. Specifically, let the rank of $\mathbf{H}_u[K/2]$ as $r_u = \mathrm{rank}(\mathbf{H}_u[K/2]) \leq N_{MS}$, and the SVD of $\mathbf{H}_u[K/2]$ is defined as $\mathbf{H}_u[K/2] = \mathbf{U}_u\mathbf{\Sigma}_u\mathbf{V}_u^H$, where $\mathbf{U}_u \in \mathbb{C}^{N_{BS}\times N_{BS}}$ and $\mathbf{V}_u \in \mathbb{C}^{N_{MS}\times N_{MS}}$ are unitary matrices, and $\mathbf{\Sigma}_u \in \mathbb{C}^{N_{BS}\times N_{MS}}$ is a diagonal matrix whose nonzero diagonal entries are the singular values of $\mathbf{H}_u[K/2]$ arranged in descending order, i.e., $\sigma_u^{(1)} \geq \sigma_u^{(2)} \geq \cdots \geq \sigma_u^{(r_u)}$. Then, $\tilde{\mathbf{F}}_{\mathrm{RF},u}$ and $\tilde{\mathbf{W}}_{\mathrm{RF},u}$ can be written as $\tilde{\mathbf{F}}_{\mathrm{RF},u} = \mathbf{V}_u(:, 1 : N_{RF}^{MS})$ and $\tilde{\mathbf{W}}_{\mathrm{RF},u}=\mathbf{U}_u\left(:, 1 : N_{RF,u}\right)$, respectively. Moreover, $\left(N_{RF,u}\right)_{u=1}^{U}$ are decided by the similar allocation framework as the previous two schemes, where we replace (26) or (29) with

$$u^* = \underset{u\in C}{\mathrm{argmax}}\ \sigma_u^{(N_{RF,u}+1)}. \tag{30}$$

Likewise, to satisfy the constant amplitude constraints, $\mathbf{F}_{\mathrm{RF},u}$ and $\mathbf{W}_{\mathrm{RF},u}$ can be obtained by extracting the phase of each element of $\tilde{\mathbf{F}}_{\mathrm{RF},u}$ and $\tilde{\mathbf{W}}_{\mathrm{RF},u}$, respectively. The more detailed steps are summarized in **Algorithm 4**.

C. OPTIMIZATION OF POWER ALLOCATION

Since all interference would have been eliminated through the low-dimensional digital beamformer completely, the power allocation of different MSs can be solved independently [49]. In order to maximize each MS's rate, the classical water-filling power allocation can be found as

$$\mathrm{P}_{u,i}[k] = \left[\frac{1}{K\lambda_u} - \frac{\sigma_n^2\left\|\mathbf{W}_u[k](:,i)\right\|^2}{\left|\mathbf{W}_u[k](:,i)^H\mathbf{H}_u[k]\mathbf{F}_u[k](:,i)\right|^2}\right]_+ \tag{31}$$

where λ_u is chosen to satisfy the total transmitted power constraint for each MS, and $[x]_+ = \max(0, x)$.

D. BENCHMARK SCHEMES

In this subsection, one fully-digital and another three hybrid designs based on the existing algorithms are developed as benchmark schemes for comparison. In these hybrid designs, we will mainly pay attention to the analog beamforming design, and a similar process as in **Algorithm 1** is adopted for the digital beamforming design.

1) FULLY-DIGITAL BEAMFORMING

This scheme is an extended version of the uplink BD mentioned in [47], which incorporates the DSA idea to further improve the performance. Although the MSs have as many RF chains as antenna elements in the fully-digital structure, each MS is restricted to assign at most N_{RF}^{MS} data streams for a fair comparison. We replace $\bar{\mathbf{H}}_u[k]$ with $\mathbf{H}_u[k]$ and carry out (9) and (10) such that the original MU MIMO channel becomes U parallel SU MIMO channels. Owing to the channel hardening effect [43], [44], for each parallel SU MIMO channel, the eigen-channel gains over the whole spectrum are approximately the same; therefore it is beneficial to simplifying the resource allocation. By modifying *Initial RF chains allocation stage* described in Section III-B to determine $n_{s,u}$, we only take the information of the eigen-channel gains on one subcarrier to create the new selection rule and replace $N_{RF,u}$ and N_{RF}^{BS} with $n_{s,u}$ and N_s, respectively. Then, the fully-digital precoder $\mathbf{F}_{\mathrm{FD},u}[k]$ and the combiner $\mathbf{W}_{\mathrm{FD},u}[k]$ are computed using (12) and (13).

2) MODIFIED AVERAGE CHANNEL MATRIX DECOMPOSITION (ACMD) [32]

Based on the proposed idea of [32], the analog precoder of the u-th MS $\mathbf{F}_{\mathrm{RF},u}$ can be designed as the phase of the right singular matrix corresponding to the largest N_{RF}^{MS} singular values of $\frac{1}{K}\sum_{k=1}^{K}\mathbf{H}_u[k]$. For the analog combiner $\mathbf{W}_{\mathrm{RF}}$, We determine the number of RF chains ($N_{RF,u}$) and transmitted data streams ($n_{s,u}$) for all served MSs according to the singular values of $\frac{1}{K}\sum_{k=1}^{K}\mathbf{H}_u[k]$ in descending order for each MS, using the aforementioned allocation framework described in Section III-B. Then, the columns of $\mathbf{W}_{\mathrm{RF},u}$ can be obtained from the phase of the left singular matrix corresponding to the largest $N_{RF,u}$ singular values of $\frac{1}{K}\sum_{k=1}^{K}\mathbf{H}_u[k]$.

3) MODIFIED ALTERNATING OPTIMIZATION BASED ON PHASE PURSUIT (ALTER-PP) [50]

Inspired by [16], [31], [50], and [51], the hybrid precoder design problem for the u-th MS is reformulated as

$$\begin{aligned}\min_{\mathbf{F}_{\mathrm{RF},u},(\mathbf{F}_{\mathrm{BB},u[k]})_{k=1}^{K}} \quad & \sum_{k=1}^{K}\left\|\mathbf{F}_{\mathrm{FD},u}[k] - \mathbf{F}_{\mathrm{RF},u}\mathbf{F}_{\mathrm{BB},u}[k]\right\|_{\mathrm{F}}^2 \\ \text{s.t.} \quad & \left|\mathbf{F}_{\mathrm{RF},u}(m,n)\right| = 1/\sqrt{N_{MS}}, \forall m, n,\end{aligned} \tag{32}$$

where $\mathbf{F}_{\mathrm{FD},u}[k]$ is the fully-digital precoder of the u-th MS at the k-th subcarrier, which is obtained from the aforementioned fully-digital beamforming scheme. The above formulation of the hybrid precoder design problem is exactly the same as that of the problem in [50], so we can directly apply Alter-PP algorithm to get the hybrid precoders. Note that this algorithm can also be used to design the hybrid combiner ($\mathbf{W}_{\mathrm{RF}}$, $(\mathbf{W}_{\mathrm{BB}}[k])_{k=1}^{K}$). However, we only obtain a near-optimal solution now, so residual interference still exists. To tackle this problem, based on the idea of [31] and [51], apart from the original $\mathbf{F}_{\mathrm{BB},u}[k]$ and $\mathbf{W}_{\mathrm{BB}}[k]$, we design another digital precoder for each MS ($\mathbf{F}_{\mathrm{bb},u}[k]$) and digital combiner ($\mathbf{W}_{\mathrm{bb}}[k]$) to cancel the residual interference. Specifically, we define an equivalent channel for the u-th MS at the k-th subcarrier as $\hat{\mathbf{H}}_{\mathrm{eq},u}[k] = \mathbf{W}_{\mathrm{BB}}^H[k]\mathbf{W}_{\mathrm{RF}}^H\mathbf{H}_u[k]\mathbf{F}_{\mathrm{RF},u}\mathbf{F}_{\mathrm{BB},u}[k]$. Then, $\bar{\mathbf{H}}_u[k]$ is replaced with $\hat{\mathbf{H}}_{\mathrm{eq},u}[k]$ such that (9), (10), (12) and (13) are employed to obtain $\mathbf{F}_{\mathrm{bb},u}[k]$ and $\mathbf{W}_{\mathrm{bb}}[k]$. Finally, the complete hybrid

TABLE 3. Complexity comparison.

	Analog	Digital
TUMD	$\mathcal{O}\left(U\left(2KN_{BS}N_{MS}N_{RF}^{MS}+\min\left\{{N_{BS}}^2KN_{RF}^{MS},N_{BS}K^2(N_{RF}^{MS})^2\right\}\right)\right)$	$\mathcal{O}\left(UKN_{BS}N_{RF}^{MS}(N_{RF}^{BS}+N_{MS})\right)$
SCCMD	$\mathcal{O}\left(U\left(N_{cl}N_{ray}\right)^2\right)$	$\mathcal{O}\left(UKN_{BS}N_{RF}^{MS}(N_{RF}^{BS}+N_{MS})\right)$
Modified SCCMD	$\mathcal{O}\left(UN_{BS}{N_{MS}}^2\right)$	$\mathcal{O}\left(UKN_{BS}N_{RF}^{MS}(N_{RF}^{BS}+N_{MS})\right)$
Modified ACMD	$\mathcal{O}\left(UN_{BS}{N_{MS}}^2\right)$	$\mathcal{O}\left(UKN_{BS}N_{RF}^{MS}(N_{RF}^{BS}+N_{MS})\right)$
Modified Alter-PP	$\mathcal{O}\left(UK(U-1)^2N_{BS}{N_{MS}}^2\right)$	$\mathcal{O}\left(UKN_{BS}N_{RF}^{MS}(N_{RF}^{BS}+N_{MS})+UKN_{RF}^{BS}n_s(N_S+N_{RF}^{MS})\right)$
Modified IGLRAM	$\mathcal{O}\left(I\left({N_{BS}}^3+U{N_{MS}}^3+UK(N_{BS}+N_{MS})(N_{BS}N_{RF}^{MS}+N_{MS}N_{RF}^{BS})\right)\right)$	$\mathcal{O}(UKN_{BS}N_{RF}^{MS}(N_{RF}^{BS}+N_{MS})+UN_{RF}^{BS}(N_{RF}^{MS})^2)$
Fully-digital	Not Involved	$\mathcal{O}\left(UK(U-1)^2N_{BS}{N_{MS}}^2\right)$

precoder of the u-th MS and the hybrid combiner are given by $\mathbf{F}_{\text{AltPP},u}[k]=\mathbf{F}_{\text{RF},u}\mathbf{F}_{\text{BB},u}[k]\,\mathbf{F}_{\text{bb},u}[k]$ and $\mathbf{W}_{\text{AltPP}}[k]=\mathbf{W}_{\text{RF}}\mathbf{W}_{\text{BB}}[k]\,\mathbf{W}_{\text{bb}}[k]$, respectively.

4) Modified Iterative Generalized Low Rank Approximation of Matrices (IGLRAM) [52]: In this design, we first formulate the analog beamforming design problem as

$$\max_{(\tilde{\mathbf{F}}_{\text{RF},u})_{u=1}^{U},\tilde{\mathbf{W}}_{\text{RF}}}\quad\sum_{u=1}^{U}\sum_{k=1}^{K}\left\|\tilde{\mathbf{W}}_{\text{RF}}^H\mathbf{H}_u[k]\tilde{\mathbf{F}}_{\text{RF},u}\right\|_{\text{F}}^2,\tag{33}$$

where $\tilde{\mathbf{W}}_{\text{RF}}$ is an unconstrained analog combiner at BS. Using the similar procedures in [52], this objective function is evaluated iteratively by updating $\tilde{\mathbf{W}}_{\text{RF}}$ and $\left(\tilde{\mathbf{F}}_{\text{RF},u}\right)_{u=1}^{U}$ so that $\sum_{u=1}^{U}\sum_{k=1}^{K}\left\|\tilde{\mathbf{W}}_{\text{RF}}^H\mathbf{H}_u[k]\tilde{\mathbf{F}}_{\text{RF},u}\right\|_{\text{F}}^2$ is maximized. After this iterative process converges, the phases of $\left(\tilde{\mathbf{F}}_{\text{RF},u}\right)_{u=1}^{U}$ and $\tilde{\mathbf{W}}_{\text{RF}}$ are extracted to satisfy the constant amplitude constraints. To determine $n_{s,u}$, the modifications of *Fully-digital beamforming* mentioned before are made, but we need to replace the selection rule according to the singular values of $\mathbf{W}_{\text{RF}}^H\mathbf{H}_u[K/2]\mathbf{F}_{\text{RF},u}$ in descending order for each MS.

IV. COMPUTATIONAL COMPLEXITY

In this section, the complexity analysis of the proposed hybrid beamforming designs is provided and the comparison is made with the benchmark schemes in Section III-D. We assume that each MS has the same number of transmitted data streams n_s for simplification.

We first evaluate the complexity of our three proposed analog beamforming designs. For TUMD described in **Algorithm 2**, the complexity mainly comes from three parts. In line 3, the EVD of $\mathbf{H}_u^{(l)^H}\mathbf{H}_u^{(l)}$ can be equivalently achieved by applying SVD to $\mathbf{H}_u^{(l)}\in\mathbb{C}^{(KN_{BS})\times N_{MS}}$. Only N_{RF}^{MS} singular vectors corresponding to the N_{RF}^{MS} largest singular values are computed to obtain $\mathbf{F}_{\text{RF},u}$, so its complexity is $\mathcal{O}\left(KN_{BS}N_{MS}N_{RF}^{MS}\right)$ [53]. After $\mathbf{F}_{\text{RF},u}$ has been designed, the computation of $\mathbf{H}_{eq,u}^{(h)}$ in line 5 requires the complexity of $\mathcal{O}\left(KN_{BS}N_{MS}N_{RF}^{MS}\right)$. The last one originates from computing the EVD of $\mathbf{H}_{eq,u}^{(h)}\mathbf{H}_{eq,u}^{(h)^H}$ in line 6. It can be equivalently achieved by applying SVD to $\mathbf{H}_{eq,u}^{(h)}\in\mathbb{C}^{N_{BS}\times(KN_{RF}^{MS})}$ whose complexity is $\mathcal{O}\left(\min\left\{N_{BS}^2KN_{RF}^{MS},N_{BS}K^2\left(N_{RF}^{MS}\right)^2\right\}\right)$ [54]. The above operations are performed U times due to U MSs, hence the overall complexity is $\mathcal{O}\left(U\left(2KN_{BS}N_{MS}N_{RF}^{MS}+\min\left\{N_{BS}^2KN_{RF}^{MS},N_{BS}K^2\left(N_{RF}^{MS}\right)^2\right\}\right)\right)$. For *SCCMD* described in **Algorithm 3**, the corresponding complexity is dominated by U sorting operations with complexity $\mathcal{O}\left(U\left(N_{cl}N_{ray}\right)^2\right)$. For *Modified SCCMD* described in **Algorithm 4**, the main complexity in computing U times of SVDs of $\mathbf{H}_u[K/2]\in\mathbb{C}^{N_{BS}\times N_{MS}}$ is $\mathcal{O}\left(UN_{BS}{N_{MS}}^2\right)$.

In our proposed digital beamforming design described in **Algorithm 1**, $\bar{\mathbf{H}}_u[k]=\mathbf{W}_{\text{RF}}^H\mathbf{H}_u[k]\mathbf{F}_{\text{RF},u}$ is first computed, which has the complexity of $\mathcal{O}\left(N_{BS}N_{RF}^{MS}\left(N_{RF}^{BS}+N_{MS}\right)\right)$. Then, the complexity of $\bar{\bar{\mathbf{H}}}_u[k]=\bar{\mathbf{H}}_u[k]\,\hat{\mathbf{F}}_u[k]$ arises from the computation of $\hat{\mathbf{F}}_u[k]$ and matrix multiplication, yielding the complexity of $\mathcal{O}\left(n_sN_{RF}^{MS}N_{RF}^{BS}\right)$. In order to obtain the orthogonal bases of the left null space of $\check{\mathbf{H}}_u[k]$ (denoted as $\check{\mathbf{U}}_{u2}[k]$), the complexity of $\mathcal{O}\left(N_{RF}^{BS}\left(N_s-n_s\right)^2\right)$ is required for performing the SVD of $\check{\mathbf{H}}_u[k]$ with dimension $N_{RF}^{BS}\times(N_s-n_s)$. $\check{\mathbf{U}}_{u2}^H[k]\,\bar{\bar{\mathbf{H}}}_u[k]$ can be calculated after the above operation, and its complexity is $\mathcal{O}\left(n_s^2N_{RF}^{BS}\right)$. Then, the SVD is further applied to it such that $\ddot{\mathbf{V}}_{u1}[k]$ and $\ddot{\mathbf{U}}_{u1}[k]$ can be obtained, which leads to the complexity of $\mathcal{O}\left(n_s^3\right)$. Finally, the unnormalized digital precoder as $\tilde{\mathbf{F}}_{\text{BB},u}[k]=\hat{\mathbf{F}}_u[k]\,\ddot{\mathbf{V}}_{u1}[k]$ and the digital combiner as $\mathbf{W}_{\text{BB},u}[k]=\check{\mathbf{U}}_{u2}[k]\,\ddot{\mathbf{U}}_{u1}[k]$ are formed. Their complexities are $\mathcal{O}\left(N_{RF}^{MS}n_s^2\right)$ and $\mathcal{O}\left(N_{RF}^{BS}n_s^2\right)$, respectively. After that, the normalization step requires the complexity of $\mathcal{O}\left(N_{RF}^{MS}n_s\left(N_{MS}+1\right)\right)$. The above operations should be performed for U MSs and K subcarriers, and N_{BS} is usually much larger than N_{RF}^{MS}, N_{RF}^{BS}, and N_{MS} in our system. Therefore, the overall complexity of the digital beamforming scheme is approximately $\mathcal{O}\left(UKN_{BS}N_{RF}^{MS}\left(N_{RF}^{BS}+N_{MS}\right)\right)$.

For comparison purpose, we also evaluate the complexity of the benchmark schemes. For *Fully-digital beamforming*, the total complexity is dominated by UK times of SVDs of the matrix with dimension $N_{BS}\times N_{MS}\,(U-1)$, which is $\mathcal{O}\left(UK\,(U-1)^2\,N_{BS}{N_{MS}}^2\right)$. The complexity analysis

TABLE 4. Simulation parameters.

Parameters	Values
Channel bandwidth	50 MHz
Number of subcarriers K	16
Noise density at the BS	-159 dBm/Hz
Cell radius	100 m
Minimum distance between the BS and each MS	10 m
Number of random channel realizations	1000
Millimeter-wave frequency f_c [4], [42]	28 GHz
Antenna array	ULA
Antenna spacing d	$\frac{\lambda}{2}$
Number of clusters N_{cl} [55], [56]	3
Number of propagation paths in each clusters N_{ray}	10

of the other benchmark schemes is divided into those of analog and digital design. For *Modified ACMD*, the main computations involve the SVD of $\frac{1}{K}\sum_{k=1}^{K}\mathbf{H}_u[k]$ with a complexity of $\mathcal{O}\left(N_{BS}{N_{MS}}^2\right)$ for each MS, followed by **Algorithm 1**, which also has about a complexity of $\mathcal{O}\left(UKN_{BS}N_{RF}^{MS}\left(N_{RF}^{BS}+N_{MS}\right)\right)$ in the digital design. For *Modified Alter-PP*, it starts to construct the fully-digital solutions at each subcarrier by performing the fully-digital beamforming scheme in Section III-D, hence its complexity is also $\mathcal{O}\left(UK\left(U-1\right)^2{N_{BS}{N_{MS}}^2}\right)$, which is dominant in the analog design. The main load of the remaining steps is $\mathcal{O}\left(UKN_{BS}N_{RF}^{MS}\left(N_{RF}^{BS}+N_{MS}\right)+UKN_{RF}^{BS}n_{s,u}\left(N_S+N_{RF}^{MS}\right)\right)$ due to the fact that $UK\hat{\mathbf{H}}_{\mathrm{eq},u}[k]$ are needed. For *Modified IGLRAM*, IGLRAM algorithm has I iterations, and each iteration has $\mathcal{O}\big(N_{BS}^3+UN_{MS}^3+UK\left(N_{BS}+N_{MS}\right)\left(N_{BS}N_{RF}^{MS}+N_{MS}N_{RF}^{BS}\right)\big)$ multiplications. In general, I is usually small such as smaller than 4 to assure convergence [52]. In the digital design, **Algorithm 1** is applied again, but it additionally needs to find the singular values of $\mathbf{W}_{\mathrm{RF}}^H\mathbf{H}_u[K/2]\mathbf{F}_{\mathrm{RF},u}$ for each MS and thus requires an extra complexity of $\mathcal{O}\left(UN_{RF}^{BS}\left(N_{RF}^{MS}\right)^2\right)$.

For clarity, Table 3 lists the complexity of the hybrid beamforming designs analyzed before along with the fully-digital, and we take $U=4$, $K=16$, $N_{BS}=128$, $N_{MS}=16$, $N_{RF}^{BS}=8$, $N_{RF}^{MS}=3$, $N_S=8$, $n_s=3$ and $N_{cl}N_{ray}=30$ as an examples. It can be seen that these hybrid schemes have the similar complexity at the digital part, and thus, the main difference comes from the analog part. We can find that the complexities of *SCCMD*, *Modified SCCMD*and *Modified ACMD* are not affected by the number of subcarriers and that their complexities are lower than those of other schemes.

V. SIMULATION RESULTS

Simulation results are presented to evaluate the performance of the proposed schemes in terms of spectral efficiency. The three proposed hybrid beamforming designs integrated into the resource allocation schemes are compared to those of the fully-digital beamforming and the three modified hybrid beamforming designs introduced in Section III-D. Referring to the legends of the simulation figures, we take HBF-TUMD-UPCBD as an example. 'HBF' represents that this design is developed based on the hybrid beamforming structure. 'TUMD' and 'UPCBD' respectively represent the labels of the analog beamforming design and the digital beamforming design. Unless otherwise stated, the default values of simulation parameters are listed in Table 4. We assume that all MSs are randomly located with uniform distribution in a circular cell. To have a fair comparison, the water-filling power allocation in Section III-C is applied to each MS for all schemes. The frequency domain channel model (5) described in Section II-B is used in our simulation. Alternatively, by applying the fast Fourier transform (FFT) to a time-domain channel model, a frequency-domain channel between the BS and the u-th MS at the k-th subcarrier can be generated. The channel parameters can be found in Table 4. The AOAs/AODs obey the Laplacian distribution with uniformly distributed mean cluster angles within $\bar{\phi}_{u,c}^r\in[0,2\pi]/\bar{\phi}_{u,c}^t\in[0,2\pi]$ and angular spreads of 10 degrees within each cluster. PL_u is generated by the path loss model of the non-line-of-sight (NLOS) urban micro (UMi) street canyon scenario in 3GPP 38.901 [57].

First, we show that the spectral efficiency performance can be significantly improved by using the DSA scheme, when it is compared to the fixed streams assignment (FSA) where the fixed number of data streams is assigned to all served MSs regardless of the CSI of each MS. In Figs. 2 and 3, the total number of received data streams are $N_s=8$ and thus, for the FSA, each MS can transmit $n_{s,u}=2$ parallel data streams to the BS simultaneously. In Fig. 2, we can observe that each proposed scheme offers the considerable performance improvement when the DSA is applied. The reason is that the MSs with stronger channel gains may be assigned more data streams such that the overall spectral efficiency is maximized. It can be seen from this figure that HBF-TUMD-UPCBD and HBF-Modified SCCMD-UPCBD outperform HBF-SCCMD-UPCBD by varying the transmit power per MS whether the DSA is applied or not. Also, even though HBF-Modified_SCCMD-UPCBD only uses the center subcarrier's channel information to design the analog beamforming matrices instead of using those of all the subcarriers like HBF-TUMD-UPCBD, it still provides the pretty good performance.

In Fig. 3, we evaluate the impact of the number of propagation paths in a cluster (N_{ray}) on the spectral efficiency performance of our proposed schemes with the DSA and FSA. Regardless the values of N_{ray}, all the proposed schemes still have the considerable performance improvement when the DSA is applied. As displayed in the figure,

with the increase of N_{ray}, the performance gap between HBF-SCCMD-UPCBD and the other two proposed schemes becomes larger whether the DSA or the FSA is applied. But it is worth noting that they achieve almost the same performance when $N_{ray} = 1$. This indicates that HBF-SCCMD-UPCBD is more suitable for small valued N_{ray} scenarios. This result is primarily affected by the asymptotic orthogonality of $\boldsymbol{A}_u^r$ and $\boldsymbol{A}_u^t$. Although we consider the scenarios of practical numbers of antennas in our simulation, in single propagation path per cluster case, $\boldsymbol{A}_u^{rH}\boldsymbol{A}_u^r \approx \mathbf{I}_{N_{BS}}$ and $\boldsymbol{A}_u^{tH}\boldsymbol{A}_u^t \approx \mathbf{I}_{N_{MS}}$ are valid even without very large-scale antenna arrays at the transceiver [25].

Next, to see the performance difference among our proposed and other existing schemes, the spectral efficiency performance curves of the fully-digital beamforming and the three benchmark schemes earlier discussed are also included in the following simulation figures, and all schemes are applied with the DSA to have the competitive performance for fair comparison. In Fig. 4, we increase the number of MSs to $U = 6$ while the other parameters remain unchanged. Note that the design of fully-digital beamforming relies on the linear processing technique here, which is known to be sub-optimal for MU-MIMO systems; therefore, in certain situations, it is possible that the hybrid beamforming designs outperform the full-digital beamforming scheme [21], [24]. Even though the linear processing technique has such a drawback, it overcomes high complexity problems of nonlinear processing techniques. As revealed in Fig. 4, HBF-TUMD-UPCBD and HBF-Modified_SCCMD-UPCBD outperform the fully-digital beamforming and HBF-TUMD-UPCBD achieves the best performance in this scenario. As observed from the figure, HBF-SCCMD-UPCBD is inferior to HBF-TUMD-UPCBD and HBF-Modified_SCCMD-UPCBD but superior to HBF-Modified_Alt-PP and HBF-Modified_IGLRAM-UPCBD.

Fig. 5 shows the spectral efficiency performance of different schemes with the DSA when the numbers of MSs (U) are varied from 3 to 8, and the transmit power per MS is set to be 20dBm. In this scenario, it is observed from the figure that all schemes reach their peaks in terms of spectral efficiency at a certain U, and then their spectral efficiencies will decrease as U increases beyond the peak points. The procedure of the digital beamforming design presented in Section III-A would explain this result for the characteristics. Similar to the analysis of [58], to ensure zero inter-user interference, we have to find the left null spaces of different users, but the overlap becomes significant while the number of users is large, which results in a performance loss. Even so, in Fig. 5, we can observe that the spectral efficiencies of our proposed hybrid beamforming schemes and HBF-Modified_ACMD-UPCBD do not degrade dramatically when the number of MSs becomes larger such as greater than 7. We also see that HBF-TUMD-UPCBD achieves the best performance compared to the other schemes when the number of MSs is larger than 5.

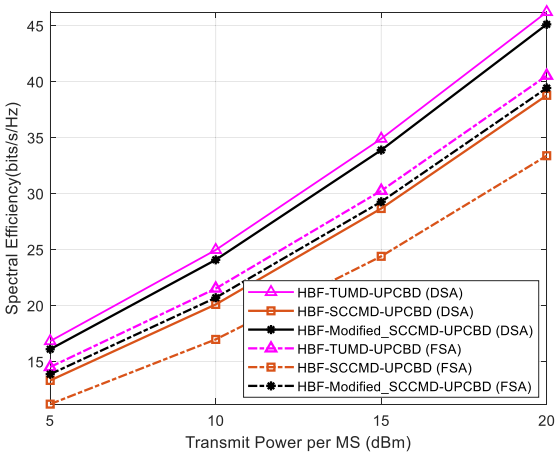

FIGURE 2. The spectral efficiency performance of our proposed hybrid beamforming schemes with the DSA and the FSA versus the transmit power per MS when $N_{BS} = 128$, $N_{MS} = 16$, $N_{RF}^{MS} = 3$, $N_s = N_{RF}^{BS} = 8$, and $U = 4$.

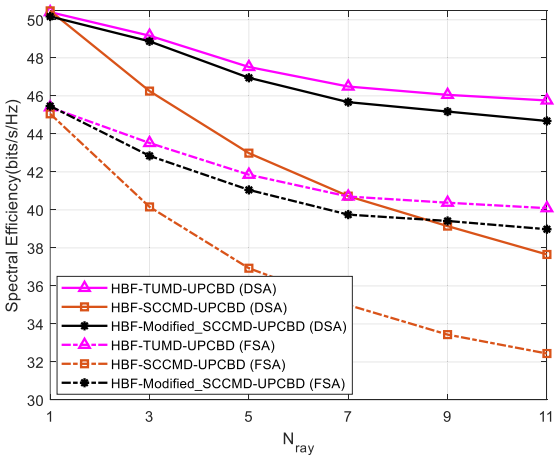

FIGURE 3. The spectral efficiency performance of our proposed hybrid beamforming schemes with the DSA and the FSA versus the number of propagation paths in a cluster (N_{ray}) when $N_{BS} = 128$, $N_{MS} = 16$, $N_{RF}^{MS} = 3$, $N_s = N_{RF}^{BS} = 8$, $U = 4$, and transmit power per MS = 20dBm.

In Fig. 6, we evaluate the spectral efficiency performance of different schemes at the transmit power per MS = 20dBm while varying the cell radius. With the same system configuration as that of Fig. 4, but the cell radiuses change at a range of 100m to 250m. Observed from the simulation results in Fig. 6, all schemes have the similar performance trend. A larger cell radius generally leads to less spectral efficiency performance due to the path loss. The HBF-TUMD-UPCBD scheme still provides the best spectral efficiency performance whenever the smaller or the larger cell radius is considered. Although the performance of HBF-SCCMD-UPCBD is poorer than those of the other two proposed schemes, its advantage is that the matrix decomposition can be avoided.

We further investigate the performance impact of different schemes on the number of BS antennas (N_{BS}) in Fig. 7. The number of BS antennas is varied at a range of 96 to 256, and the other parameters remain unchanged. It can be

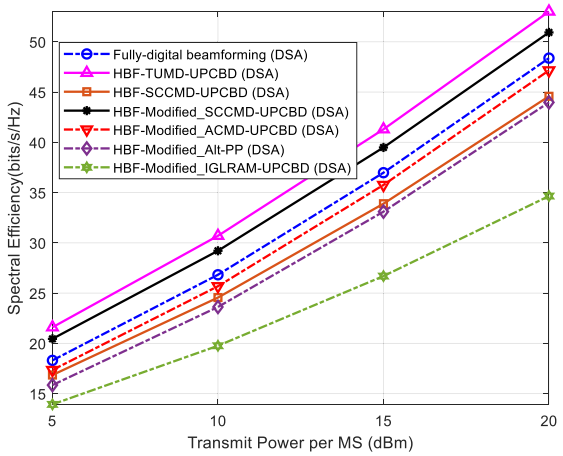

FIGURE 4. The spectral efficiency performance of our proposed hybrid beamforming and benchmark schemes with the DSA versus the transmit power per MS when $N_{BS} = 128$, $N_{MS} = 16$, $N_{RF}^{MS} = 3$, $N_s = N_{RF}^{BS} = 8$, and $U = 6$.

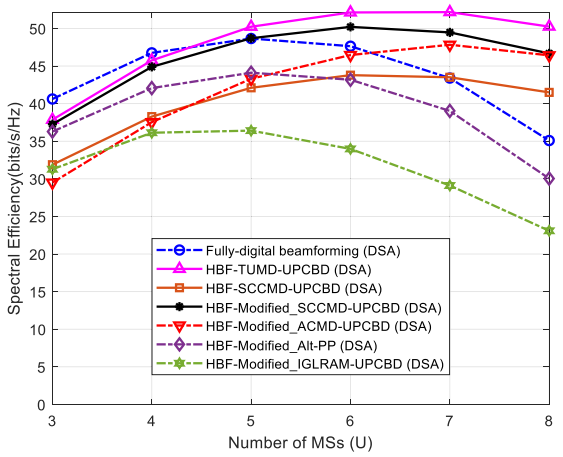

FIGURE 5. The spectral efficiency performance of our proposed hybrid beamforming and benchmark schemes with the DSA versus the number of MSs (U) when $N_{BS} = 128$, $N_{MS} = 16$, $N_{RF}^{MS} = 3$, $N_s = N_{RF}^{BS} = 8$, and transmit power per MS = 20dBm.

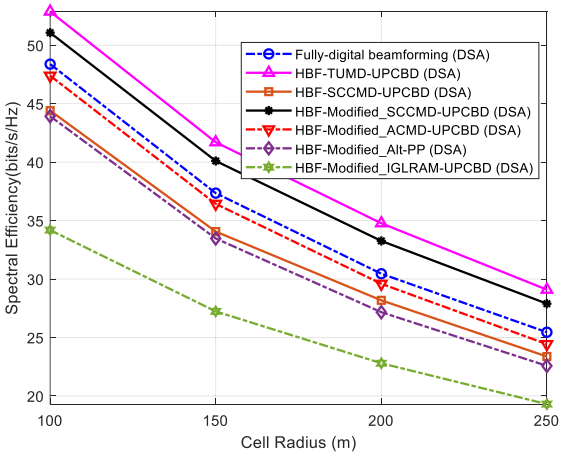

FIGURE 6. The spectral efficiency performance of our proposed hybrid beamforming and benchmark schemes with the DSA versus the cell radius when $N_{BS} = 128$, $N_{MS} = 16$, $N_{RF}^{MS} = 3$, $N_s = N_{RF}^{BS} = 8$, $U = 6$, and transmit power per MS = 20dBm.

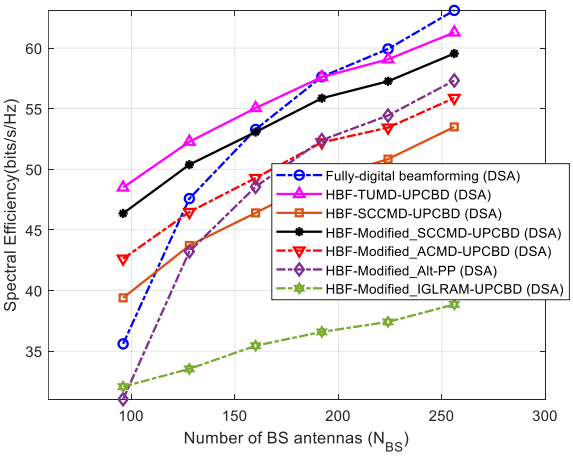

FIGURE 7. The spectral efficiency performance of our proposed hybrid beamforming and benchmark schemes with the DSA versus the number of BS antennas (N_{BS}) when $N_{MS} = 16$, $N_{RF}^{MS} = 3$, $N_s = N_{RF}^{BS} = 8$, $U = 6$, and transmit power per MS = 20dBm.

observed from this figure that the spectral efficiency performance of all schemes improves correspondingly when N_{BS} increases. This figure also shows that our proposed schemes have a considerable performance gain over the fully-digital beamforming when N_{BS} is smaller such as 96. However, we find that, as N_{BS} gradually increases, the performance of the fully-digital beamforming becomes superior to those of our proposed schemes. Although this observation indicates that the fully-digital beamforming achieves a significant performance improvement by increasing N_{BS}, it would have the heavy implementation cost and high energy consumption since more RF chains are required. Therefore, the proposed hybrid beamforming schemes with the limited RF chain configuration such as HBF-TUMD-UPCBD and HBF-Modified_SCCMD-UPCBD may be better choices for massive MIMO systems. From Figs. 4 to 7, under the various parameter settings, it is worth mentioning that the performance of HBF-Modified_Alt-PP is worse than that of the fully-digital beamforming and they have the similar performance trend. This is because the performance of the HBF-Modified_Alt-PP depends on that of the fully-digital beamforming.

VI. CONCLUSION

In this paper, we propose three hybrid beamforming designs with DSA for the uplink mmWave MU massive MIMO-OFDM system to maximize the overall spectral efficiency for the formulated resource allocation problem. Our proposed algorithms perform the analog and the digital beamforming design into two separate stages. Three designs of the analog precoders and the combiner are developed, while the number of transmitted data streams for each MS is dynamically assigned to achieve better performance. Based on the ideas of the BD and the coordinated transmit-receive

processing, we design the digital precoder and the combiner according to the equivalent baseband channel to eliminate the inter-user interference and the inter-stream interference completely.

In the performance comparison, three existing hybrid beamforming designs are slightly modified and extended as benchmark schemes to be applied to our system scenario setting for the problem under consideration. The simulation results show that the spectral efficiency of the proposed schemes has significant improvement by dynamically adjusting the number of data streams for each MS according to the CSI in comparison with the FSA. It is also shown that the proposed hybrid beamforming designs can achieve a pretty excellent performance, except the HBF-SCCMD-UPCBD, compared to those of the benchmark schemes. It can even outperform the fully-digital design in some situations, especially when the number of served MSs is large. Moreover, although the HBF-SCCMD-UPCBD performs worse than the other proposed schemes, it is worth noting that its computational complexity is greatly reduced.

REFERENCES

[1] S. K. Yong and C.-C. Chong, "An overview of multigigabit wireless through millimeter wave technology: Potentials and technical challenges," *EURASIP J. Wireless Commun. Netw.*, vol. 2007, no. 1, pp. 1–10, Dec. 2006.

[2] T. S. Rappaport, J. N. Murdock, and F. Gutierrez, "State of the art in 60-GHz integrated circuits and systems for wireless communications," *Proc. IEEE*, vol. 99, no. 8, pp. 1390–1436, Aug. 2011.

[3] R. C. Daniels and R. W. Heath, "60 GHz wireless communications: Emerging requirements and design recommendations," *IEEE Veh. Technol. Mag.*, vol. 2, no. 3, pp. 41–50, Sep. 2007.

[4] M. R. Akdeniz, Y. Liu, M. K. Samimi, S. Sun, S. Rangan, T. S. Rappaport, and E. Erkip, "Millimeter wave channel modeling and cellular capacity evaluation," *IEEE J. Sel. Areas Commun.*, vol. 32, no. 6, pp. 1164–1179, Jun. 2014.

[5] Y. Azar, G. N. Wong, K. Wang, R. Mayzus, J. K. Schulz, H. Zhao, F. Gutierrez, D. Hwang, and T. S. Rappaport, "28 GHz propagation measurements for outdoor cellular communications using steerable beam antennas in New York City," in *Proc. IEEE Int. Conf. Commun. (ICC)*, Jun. 2013, pp. 5143–5147.

[6] T. S. Rappaport, S. Sun, R. Mayzus, H. Zhao, Y. Azar, K. Wang, G. N. Wong, J. K. Schulz, M. Samimi, and F. Gutierrez, "Millimeter wave mobile communications for 5G cellular: It will work!" *IEEE Access*, vol. 1, pp. 335–349, 2013.

[7] G. R. MacCartney, J. Zhang, S. Nie, and T. S. Rappaport, "Path loss models for 5G millimeter wave propagation channels in urban microcells," in *Proc. IEEE Global Commun. Conf. (GLOBECOM)*, Dec. 2013, pp. 3948–3953.

[8] L. Lu, G. Y. Li, A. L. Swindlehurst, A. Ashikhmin, and R. Zhang, "An overview of massive MIMO: Benefits and challenges," *IEEE J. Sel. Topics Signal Process.*, vol. 8, no. 5, pp. 742–758, Oct. 2014.

[9] R. W. Heath Jr., N. González-Prelcic, S. Rangan, W. Roh, and A. M. Sayeed, "An overview of signal processing techniques for millimeter wave MIMO systems," *IEEE J. Sel. Topics Signal Process.*, vol. 10, no. 3, pp. 436–453, Apr. 2016.

[10] O. E. Ayach, S. Rajagopal, S. Abu-Surra, Z. Pi, and R. W. Heath Jr., "Spatially sparse precoding in millimeter wave MIMO systems," *IEEE Trans. Wireless Commun.*, vol. 13, no. 3, pp. 1499–1513, Mar. 2014.

[11] S. Sun, T. S. Rappaport, R. W. Heath, A. Nix, and S. Rangan, "MIMO for millimeter-wave wireless communications: Beamforming, spatial multiplexing, or both?" *IEEE Commun. Mag.*, vol. 52, no. 12, pp. 110–121, Dec. 2014.

[12] F. Rusek, D. Persson, B. K. Lau, E. G. Larsson, T. L. Marzetta, O. Edfors, and F. Tufvesson, "Scaling up MIMO: Opportunities and challenges with very large arrays," *IEEE Signal Process. Mag.*, vol. 30, no. 1, pp. 40–60, Jan. 2013.

[13] S. Kutty and D. Sen, "Beamforming for millimeter wave communications: An inclusive survey," *IEEE Commun. Surveys Tuts.*, vol. 18, no. 2, pp. 949–973, 2nd Quart., 2016.

[14] T. Gong, N. Shlezinger, S. S. Ioushua, M. Namer, Z. Yang, and Y. C. Eldar, "RF chain reduction for MIMO systems: A hardware prototype," *IEEE Syst. J.*, vol. 14, no. 4, pp. 5296–5307, Dec. 2020.

[15] D. Zhang, P. Pan, R. You, and H. Wang, "SVD-based low-complexity hybrid precoding for millimeter-wave MIMO systems," *IEEE Commun. Lett.*, vol. 22, no. 10, pp. 2176–2179, Oct. 2018.

[16] X. Yu, J.-C. Shen, J. Zhang, and K. B. Letaief, "Alternating minimization algorithms for hybrid precoding in millimeter wave MIMO systems," *IEEE J. Sel. Topics Signal Process.*, vol. 10, no. 3, pp. 485–500, Apr. 2016.

[17] Y. Wang and W. Zou, "Low complexity hybrid precoder design for millimeter wave MIMO systems," *IEEE Commun. Lett.*, vol. 23, no. 7, pp. 1259–1262, Jul. 2019.

[18] M. Alouzi, F. Chan, and C. D'Amours, "Low complexity hybrid precoding and combining for millimeter wave systems," *IEEE Access*, vol. 9, pp. 95911–95924, 2021.

[19] F. Sohrabi and W. Yu, "Hybrid digital and analog beamforming design for large-scale antenna arrays," *IEEE J. Sel. Topics Signal Process.*, vol. 10, no. 3, pp. 501–513, Apr. 2016.

[20] R. Zhang, W. Zou, Y. Wang, and M. Cui, "Hybrid precoder and combiner design for single-user mmWave MIMO systems," *IEEE Access*, vol. 7, pp. 63818–63828, 2019.

[21] W. Ni and X. Dong, "Hybrid block diagonalization for massive multiuser MIMO systems," *IEEE Trans. Commun.*, vol. 64, no. 1, pp. 201–211, Jan. 2016.

[22] X. Wu, D. Liu, and F. Yin, "Hybrid beamforming for multi-user massive MIMO systems," *IEEE Trans. Commun.*, vol. 66, no. 9, pp. 3879–3891, Sep. 2018.

[23] F. Khalid, "Hybrid beamforming for millimeter wave massive multiuser MIMO systems using regularized channel diagonalization," *IEEE Wireless Commun. Lett.*, vol. 8, no. 3, pp. 705–708, Jun. 2019.

[24] J. Zhan and X. Dong, "Interference cancellation aided hybrid beamforming for mmWave multi-user massive MIMO systems," *IEEE Trans. Veh. Technol.*, vol. 70, no. 3, pp. 2322–2336, Mar. 2021.

[25] F. Sohrabi and W. Yu, "Hybrid analog and digital beamforming for mmWave OFDM large-scale antenna arrays," *IEEE J. Sel. Areas Commun.*, vol. 35, no. 7, pp. 1432–1443, Jul. 2017.

[26] M. Ma, N. Thanh Nguyen, and M. Juntti, "Closed-form hybrid beamforming solution for spectral efficiency upper bound maximization in mmWave MIMO-OFDM systems," in *Proc. IEEE 94th Veh. Technol. Conf.*, Sep. 2021, pp. 1–5.

[27] T. Lin, J. Cong, Y. Zhu, J. Zhang, and K. B. Letaief, "Hybrid beamforming for millimeter wave systems using the MMSE criterion," *IEEE Trans. Commun.*, vol. 67, no. 5, pp. 3693–3708, May 2019.

[28] J. Du, W. Xu, C. Zhao, and L. Vandendorpe, "Weighted spectral efficiency optimization for hybrid beamforming in multiuser massive MIMO-OFDM systems," *IEEE Trans. Veh. Technol.*, vol. 68, no. 10, pp. 9698–9712, Oct. 2019.

[29] Y. Liu and J. Wang, "Low-complexity OFDM-based hybrid precoding for multiuser massive MIMO systems," *IEEE Wireless Commun. Lett.*, vol. 9, no. 3, pp. 263–266, Mar. 2020.

[30] J.-S. Jung, W.-S. Lee, Y.-R. Lee, J. Kim, and H.-K. Song, "Improved hybrid beamforming for mmWave multi-user massive MIMO," *Comput., Mater. Continua*, vol. 67, no. 3, pp. 3057–3070, 2021.

[31] H. Yuan, J. An, N. Yang, K. Yang, and T. Q. Duong, "Low complexity hybrid precoding for multiuser millimeter wave systems over frequency selective channels," *IEEE Trans. Veh. Technol.*, vol. 68, no. 1, pp. 983–987, Jan. 2019.

[32] D. Zhang, Y. Wang, X. Li, and W. Xiang, "Hybrid beamforming for downlink multiuser millimetre wave MIMO-OFDM systems," *IET Commun.*, vol. 13, no. 11, pp. 1557–1564, Jul. 2019.

[33] S. Gherekhloo, K. Ardah, and M. Haardt, "Hybrid beamforming design for downlink MU-MIMO-OFDM millimeter-wave systems," in *Proc. IEEE 11th Sensor Array Multichannel Signal Process. Workshop (SAM)*, Jun. 2020, pp. 1–5.

[34] Y. Chen, D. Chen, T. Jiang, and L. Hanzo, "Channel-covariance and angle-of-departure aided hybrid precoding for wideband multiuser millimeter wave MIMO systems," *IEEE Trans. Commun.*, vol. 67, no. 12, pp. 8315–8328, Dec. 2019.

[35] Y. Sun, H. Wang, M. Yuan, T. Zhu, and A. Kawoya, "Training-based hybrid precoding scheme for multiuser massive MIMO-OFDM," *IEEE Commun. Lett.*, vol. 25, no. 11, pp. 3729–3732, Nov. 2021.
[36] R. Chen, Z. Shen, J. G. Andrews, and R. W. Heath Jr., "Multimode transmission for multiuser MIMO systems with block diagonalization," *IEEE Trans. Signal Process.*, vol. 56, no. 7, pp. 3294–3302, Jul. 2008.
[37] Y.-U. Jang, H. M. Kwon, and Y. H. Lee, "Adaptive mode selection for multiuser MIMO downlink systems," in *Proc. IEEE 63rd Veh. Technol. Conf.*, May 2006, pp. 2003–2007.
[38] Z. Li, S. Han, and A. F. Molisch, "Optimizing channel-statistics-based analog beamforming for millimeter-wave multi-user massive MIMO downlink," *IEEE Trans. Wireless Commun.*, vol. 16, no. 7, pp. 4288–4303, Jul. 2017.
[39] G. Kwon and H. Park, "Limited feedback hybrid beamforming for multi-mode transmission in wideband millimeter wave channel," *IEEE Trans. Wireless Commun.*, vol. 19, no. 6, pp. 4008–4022, Jun. 2020.
[40] S. Wang, M. He, R. Ruby, and Y. Zhang, "SVM-based optimization on the number of data streams for massive MIMO systems," *IEEE Syst. J.*, vol. 17, no. 1, pp. 83–86, Mar. 2023.
[41] Y. Yifei and Z. Longming, "Application scenarios and enabling technologies of 5G," *China Commun.*, vol. 11, no. 11, pp. 69–79, Nov. 2014.
[42] I. A. Hemadeh, K. Satyanarayana, M. El-Hajjar, and L. Hanzo, "Millimeter-wave communications: Physical channel models, design considerations, antenna constructions, and link-budget," *IEEE Commun. Surveys Tuts.*, vol. 20, no. 2, pp. 870–913, 2nd Quart., 2018.
[43] E. G. Larsson, O. Edfors, F. Tufvesson, and T. L. Marzetta, "Massive MIMO for next generation wireless systems," *IEEE Commun. Mag.*, vol. 52, no. 2, pp. 186–195, Feb. 2014.
[44] E. Björnson, E. G. Larsson, and T. L. Marzetta, "Massive MIMO: Ten myths and one critical question," *IEEE Commun. Mag.*, vol. 54, no. 2, pp. 114–123, Feb. 2016.
[45] Z. Pi and F. Khan, "An introduction to millimeter-wave mobile broadband systems," *IEEE Commun. Mag.*, vol. 49, no. 6, pp. 101–107, Jun. 2011.
[46] Q. H. Spencer, A. L. Swindlehurst, and M. Haardt, "Zero-forcing methods for downlink spatial multiplexing in multiuser MIMO channels," *IEEE Trans. Signal Process.*, vol. 52, no. 2, pp. 461–471, Feb. 2004.
[47] L. Arévalo, R. C. de Lamare, M. Haardt, and R. Sampaio-Neto, "Uplink block diagonalization for massive MIMO-OFDM systems with distributed antennas," in *Proc. IEEE 6th Int. Workshop Comput. Adv. Multi-Sensor Adapt. Process. (CAMSAP)*, Dec. 2015, pp. 389–392.
[48] P.-H. Lee and Y.-P. Lin, "Hybrid MIMO-OFDM for downlink multi-user communications over millimeter channels with no instantaneous feedback," in *Proc. IEEE Int. Symp. Circuits Syst. (ISCAS)*, May 2019, pp. 1–5.
[49] B. Farhang-Boroujeny, Q. Spencer, and L. Swindlehurst, "Layering techniques for space-time communication in multi-user networks," in *Proc. IEEE 58th Veh. Technol. Conf.*, Oct. 2003, pp. 1339–1342.
[50] R. Zhang, W. Zou, Y. Wang, M. Cui, and X. Sun, "Alternate hybrid precoding algorithm for wideband millimetre wave massive MIMO systems," *IET Commun.*, vol. 14, no. 8, pp. 1261–1267, May 2020.
[51] X. Yu, J. Zhang, and K. B. Letaief, "Alternating minimization for hybrid precoding in multiuser OFDM mmWave systems," in *Proc. 50th Asilomar Conf. Signals, Syst. Comput.*, Nov. 2016, pp. 281–285.
[52] N. Song, T. Yang, and H. Sun, "Overlapped subarray based hybrid beamforming for millimeter wave multiuser massive MIMO," *IEEE Signal Process. Lett.*, vol. 24, no. 5, pp. 550–554, May 2017.
[53] G. H. Golub and C. F. Van Loan, *Matrix Computations*, 4th ed. Baltimore, MD, USA: John Hopkins Uni. Press, 2013.
[54] M. Holmes, A. Gray, and C. Isbell, "Fast SVD for large-scale matrices," in *Proc. Workshop Efficient Mach. Learn. NIPS*, 2007, pp. 249–252.
[55] S. Wu, S. Hur, K. Whang, and M. Nekovee, "Intra-cluster characteristics of 28 GHz wireless channel in urban micro street canyon," in *Proc. IEEE Global Commun. Conf. (GLOBECOM)*, Dec. 2016, pp. 1–6.
[56] J. Ko, Y.-J. Cho, S. Hur, T. Kim, J. Park, A. F. Molisch, K. Haneda, M. Peter, D.-J. Park, and D.-H. Cho, "Millimeter-wave channel measurements and analysis for statistical spatial channel model in in-building and urban environments at 28 GHz," *IEEE Trans. Wireless Commun.*, vol. 16, no. 9, pp. 5853–5868, Sep. 2017.
[57] *Technical Specification Group Radio Access Network; Study on Channel Model for Frequencies From 0.5 to 100 GHz (Release 16)*, 3GPP, document TR 38.901, 2019.
[58] V. Stankovic and M. Haardt, "Generalized design of multi-user MIMO precoding matrices," *IEEE Trans. Wireless Commun.*, vol. 7, no. 3, pp. 953–961, Mar. 2008.

HSIN-HSIANG TSENG received the B.S. degree in electrical engineering from Chang Gung University, Taoyuan City, Taiwan, in 2019, and the M.S. degree in communication engineering from National Central University, Taoyuan City, in 2022. His research interests include MIMO communication techniques, resource allocation for wireless communication systems, and signal processing algorithm designs for mmWave systems.

YUNG-FANG CHEN (Member, IEEE) received the B.S. degree in computer science and information engineering from National Taiwan University, Taipei City, Taiwan, in 1990, the M.S. degree in electrical engineering from the University of Maryland, College Park, MD, USA, in 1994, and the Ph.D. degree in electrical engineering from Purdue University, West Lafayette, IN, USA, in 1998. From 1998 to 2000, he was with Lucent Technologies, Whippany, NJ, USA, where he was with the CDMA Radio Technology Performance Group. Since 2000, he has been a Faculty Member with the Department of Communication Engineering, National Central University, Taoyuan City, Taiwan, where he is currently a Professor. From 2017 to 2020, he was the Chairperson of the Department of Communication Engineering, National Central University. From 2021 to 2022, he was the Vice Dean of the College of Electrical Engineering and Computer Science. His research interests include resource management algorithm designs for communication systems and signal processing algorithm designs for wireless communication systems.

SHU-MING TSENG (Member, IEEE) received the B.S. degree in electrical engineering from National Tsing Hua University, Taiwan, in 1994, and the M.S. and Ph.D. degrees in electrical engineering from Purdue University, West Lafayette, IN, USA, in 1995 and 1999, respectively. From 1999 to 2001, he was with the Department of Electrical Engineering, Chang Gung University, Taiwan. Since 2001, he has been with the Department of Electronic Engineering, National Taipei University of Technology, Taipei City, Taiwan, where he has been a Professor, since 2007. He is currently the author of 46 SCI journal articles. His research interests include NOMA, MU-MIMO, OFDMA, deep learning-based radio resource allocation, cross-layer optimization for video transmission, network performance evaluation, software-defined radio, and optical systems. He has been serving as an Editor for *KSII Transactions on Internet and Information Systems*, indexed in SCI, since 2013.